

# Revisiting rescattering contributions to $\bar{B}_{(s)} \rightarrow D_{(s)}^{(*)} M$ decays

**Motoi Endo,<sup>a,b,c</sup> Syuhei Iguro,<sup>c</sup> and Satoshi Mishima<sup>a</sup>**

<sup>a</sup>*Theory Center, IPNS, KEK, Tsukuba 305-0801, Japan*

<sup>b</sup>*The Graduate University of Advanced Studies (Sokendai), Tsukuba 305-0801, Japan*

<sup>c</sup>*Kavli Institute for the Physics and Mathematics of the Universe, University of Tokyo, Kashiwa 277-8583, Japan*

*E-mail:* [motoi.endo@kek.jp](mailto:motoi.endo@kek.jp), [syuhei.iguro@ipmu.jp](mailto:syuhei.iguro@ipmu.jp),  
[satoshi.mishima@kek.jp](mailto:satoshi.mishima@kek.jp)

**ABSTRACT:** Motivated by the reported discrepancies between experimental data and Standard Model predictions for the branching ratios of the color-allowed decays  $\bar{B}^0 \rightarrow D^{(*)+} K^-$  and  $\bar{B}_s^0 \rightarrow D_s^{(*)+} \pi^-$ , we study final-state rescattering effects on  $\bar{B}_{(s)} \rightarrow D_{(s)}^{(*)} P$  and  $\bar{B}_{(s)} \rightarrow D_{(s)} V$ , where  $P$  ( $V$ ) is a light pseudoscalar (vector) meson. We consider quasi-elastic rescatterings in the framework of  $SU(3)$  and  $U(3)$  flavor symmetries, and find that the effects cannot explain the measured branching ratios of the color-allowed and color-suppressed decays simultaneously. We also perform global fits to the  $\bar{B}_{(s)} \rightarrow D_{(s)}^{(*)} P$  and  $\bar{B}_{(s)} \rightarrow D_{(s)} V$  data, allowing for new physics contributions to the Wilson coefficient  $a_1$  associated with the color-allowed tree amplitudes. It is shown that the fits prefer a downward shift of  $\mathcal{O}(10\%)$  in  $a_1$  even in the presence of the quasi-elastic rescattering contributions.

---

## Contents

|          |  |           |
|----------|--|-----------|
| <b>1</b> | <b>Introduction</b>  | <b>1</b>  |
| <b>2</b> | <b>Theoretical framework</b>                                   | <b>3</b>  |
| 2.1      | Decay amplitudes   | 3         |
| 2.2      | Quasi-elastic rescattering                                     | 7         |
| <b>3</b> | <b>Numerical analysis</b>                                      | <b>10</b> |
| 3.1      | Color-allowed decays   | 10        |
| 3.2      | Rescattering between color-allowed and color-suppressed decays | 12        |
| 3.3      | Global analysis  | 15        |
| <b>4</b> | <b>Summary</b>   | <b>18</b> |
| <b>A</b> | <b>Fit results</b>   | <b>19</b> |

---

## 1 Introduction

Two-body hadronic  $B$  decays into a heavy-light final state  $\bar{B}_{(s)} \rightarrow D_{(s)}^{(*)} M$ , where  $M$  is a light meson, have played an important role in testing the factorization hypothesis [1]. In  $\bar{B}_{(s)}^0 \rightarrow D_{(s)}^+ \pi^-$  and  $\bar{B}_{(s)}^0 \rightarrow D_{(s)}^+ K^-$  decays, which are dominated by the so-called color-allowed tree amplitude, the hypothesis is expected to work well, since contributions from a gluon exchange between the light meson emitted from the weak vertex and the soft spectator quark in a heavy meson are power suppressed in the heavy-quark limit. Moreover, they have no penguin contribution. For these decays the factorization theorem was proved at the leading power in the heavy-quark expansion with the QCD factorization (QCDF) approach [2] and with the soft-collinear effective theory (SCET) [3]. There are great improvements in theoretical calculations of the color-allowed tree amplitude in recent years, which enable us to study possible contributions to these decays from new-physics (NP) beyond the Standard Model (SM).

The branching ratios of  $\bar{B}_{(s)}^0 \rightarrow D_{(s)}^{(*)+} \pi^-$  and  $\bar{B}_{(s)}^0 \rightarrow D_{(s)}^{(*)+} K^-$  are calculated in QCDF to next-to-next-to-leading order (NNLO) accuracy [4]. They have recently been updated in ref. [5] with new determinations of  $\bar{B}_{(s)} \rightarrow D_{(s)}^{(*)}$  form factors in the heavy-quark expansion up to  $\mathcal{O}(\Lambda_{\text{QCD}}^2/m_c^2)$  [6]. The updated predictions for the branching ratios show a tension with the experimental measurements with a significance of the  $4.4\sigma$  level [5].<sup>1</sup>

The tension requires a downward shift of 10% in the  $b \rightarrow c\bar{u}q$  amplitude with  $q$  being  $d$  or  $s$ , which might be caused by NP.<sup>2</sup> It is shown in ref. [9] that the tension can be reduced

---

<sup>1</sup>Similar results are obtained in ref. [7] with different inputs.

<sup>2</sup>Implication of CP-violating NP phases is studied in ref. [8].

partly by introducing a new vector boson  $W'$  without conflicting with narrow resonance searches at the Large Hadron Collider (LHC).<sup>3</sup>

On the other hand, the experimental data for the branching ratios of  $\bar{B}^0 \rightarrow D^{(*)+}\pi^-$ ,  $\bar{B}^0 \rightarrow D^{(*)0}\pi^0$  and  $B^- \rightarrow D^{(*)0}\pi^-$  indicate a failure of the naive factorization [10, 11].<sup>4</sup> Here  $\bar{B}^0 \rightarrow D^{(*)0}\pi^0$  is dominated by the color-suppressed tree amplitude, while  $B^- \rightarrow D^{(*)0}\pi^-$  has both the color-allowed and color-suppressed tree amplitudes. For  $a_1$  and  $a_2$  being the Wilson coefficients associated with the color-allowed and color-suppressed tree amplitudes, respectively, a fit to the data prefers a larger  $|a_2|$  compared to those extracted from  $\bar{B} \rightarrow J/\psi \bar{K}^{(*)}$  and  $\bar{B} \rightarrow \psi(2S) \bar{K}^{(*)}$  with a sizable relative phase between  $a_1$  and  $a_2$ . Similar results can also be obtained from other  $\bar{B}_{(s)} \rightarrow D_{(s)}^{(*)}M$  processes [14–16]. The relative phase between  $a_1$  and  $a_2$  implies that final-state interactions (FSI) are significant in the color-suppressed modes.<sup>5</sup>

It is however difficult to calculate the FSI effects in  $\bar{B}_{(s)} \rightarrow D_{(s)}^{(*)}M$  from first principles.<sup>6</sup> In SCET, the FSI contributions in the color-suppressed decays are factorized into soft factors [20, 21], which have to be calculated in non-perturbative methods or extracted from data. Non-factorizable contributions from a single soft-gluon exchange are estimated with the light-cone QCD sum rules (LCSR) for the color-allowed decays [5] and the color-suppressed decays [22, 23], and the size of them for the former (latter) is found to be insignificant (significant) compared to the factorizable ones. Also the rescattering of the final-state mesons are studied with various models [24–36].

It is pointed out in ref. [24] using the Regge approach that the final-state rescattering effects do not vanish in the large  $b$ -quark mass limit. On the other hand, in the QCDF approach, the rescattering effects are found to be suppressed in the heavy-quark limit [2]. Hence the suppression could be understood by a systematic cancellation among all intermediate hadronic states [2, 26]. Nonetheless, the rescattering effects may remain sizable, since the  $b$ -quark mass is not infinite in reality.

In this paper we study the *quasi-elastic* rescattering contributions to the  $\bar{B}_{(s)} \rightarrow D_{(s)}^{(*)}M$  decays, following the framework developed in refs. [27, 34, 35]. The elastic  $D\pi \rightarrow D\pi$  rescattering picture is extended to quasi-elastic  $D^{(*)}P \rightarrow D^{(*)}P$  and  $DV \rightarrow DV$  rescatterings by based on  $SU(3)$  and  $U(3)$  flavor symmetries, where  $P$  and  $V$  represent the pseudoscalar  $SU(3)$  octet and the vector  $U(3)$  nonet, respectively. We assume that inelastic-rescattering contributions are suppressed, and examine the question whether the quasi-elastic rescattering contributions can resolve the tensions between the theoretical predictions and the experimental data for the color-allowed decays. The analyses in refs. [27, 34, 35] are updated with latest theoretical and experimental information. In particular, the Wilson coefficient  $a_1$  at NNLO [4] and the  $\bar{B}_{(s)} \rightarrow D_{(s)}^{(*)}$  form factors at  $\mathcal{O}(\Lambda_{\text{QCD}}^2/m_c^2)$  [37] are employed to

<sup>3</sup>A model-independent NP analysis has also been carried out in ref. [7].

<sup>4</sup>A different conclusion was obtained in refs. [12, 13].

<sup>5</sup>In the PQCD approach based on the  $k_T$  factorization, the larger  $|a_2|$  with the sizable phase is explained by spectator-scattering contributions [17, 18].

<sup>6</sup>The FSI effects in heavy meson decays were explored first for the charmed meson decays in ref. [19] using QCD sum rules.

make the calculation of the color-allowed tree amplitude more reliable.<sup>7</sup>

This paper is organized as follows. In section 2 the theoretical framework for calculating decay amplitudes is described under the presence of the quasi-elastic rescattering. In section 3 numerical analysis of the rescattering effects in the color-allowed decays is presented. Finally, the section 4 is devoted to conclusions and discussion. Besides, appendix A contains some details of numerical results.

## 2 Theoretical framework

In this section the theoretical framework for calculating decay amplitudes is briefly introduced with quasi-elastic rescattering contributions. The decays of  $\bar{B} \rightarrow DP$ ,  $\bar{B} \rightarrow D^*P$ , and  $\bar{B} \rightarrow DV$  with  $b \rightarrow c\bar{u}q$  transitions are studied, where  $q$  is  $d, s$ , and  $P$  ( $V$ ) stands for a light pseudoscalar (vector) meson.<sup>8</sup>

### 2.1 Decay amplitudes

The weak effective Hamiltonian relevant for the current study consists only of the following tree operators:

$$\mathcal{H}_W = \frac{4G_F}{\sqrt{2}} \sum_{q=d,s} V_{cb}V_{uq}^* (C_1 \mathcal{O}_1^q + C_2 \mathcal{O}_2^q) + \text{h.c.}, \quad (2.1)$$

where  $V_{ij}$  are the Cabibbo-Kobayashi-Maskawa (CKM) matrix elements [40, 41]. The local operators are defined in the Chetyrkin-Misiak-Münz (CMM) basis [42, 43] as

$$\mathcal{O}_1^q = (\bar{c}\gamma^\mu T^a P_L b)(\bar{q}\gamma_\mu T^a P_L u), \quad (2.2)$$

$$\mathcal{O}_2^q = (\bar{c}\gamma^\mu P_L b)(\bar{q}\gamma_\mu P_L u), \quad (2.3)$$

where  $P_L = (1 - \gamma_5)/2$ , and  $T^a$  is a generator of  $SU(3)$ . Suppose that there is no CP-violating phase in  $\mathcal{H}_W$ <sup>9</sup>, the time-reversal invariance of  $\mathcal{H}_W$  leads to

$$\langle i; \text{out} | \mathcal{H}_W | \bar{B} \rangle^* = \sum_j S_{ji}^* \langle j; \text{out} | \mathcal{H}_W | \bar{B} \rangle, \quad (2.4)$$

where the strong scattering  $S$ -matrix element  $S_{ji}$  is defined in terms of *in* and *out* states as  $S_{ji} = \langle j; \text{out} | i; \text{in} \rangle$ . The solution of this relation is given by  $\langle i; \text{out} | \mathcal{H}_W | \bar{B} \rangle = \sum_j S_{ij}^{1/2} \mathcal{A}_j^0$ , where  $\mathcal{A}_j^0$  is real [26]. A decay amplitude with FSI, denoted as  $\mathcal{A}_i^{\text{FSI}} = \langle i; \text{out} | \mathcal{H}_W | \bar{B} \rangle$ , is given by

$$\mathcal{A}_i^{\text{FSI}} = \sum_j S_{ij}^{1/2} \mathcal{A}_j^0, \quad (2.5)$$

---

<sup>7</sup>It is assumed that the  $SU(3)$  flavor symmetry holds between the  $\bar{B} \rightarrow D^{(*)}$  and  $\bar{B}_s \rightarrow D_s^{(*)}$  form factors as suggested in the result of refs. [6, 38].

<sup>8</sup>We do not consider  $\bar{B} \rightarrow D^*V$  in this paper, since experimental uncertainties are large [39].

<sup>9</sup>Note that the CP-violating phase in the CKM matrix is irrelevant in the current study.

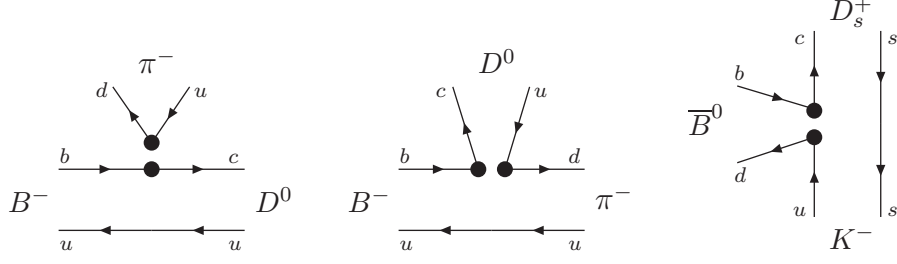


**Figure 1.** Representative diagrams of the  $b \rightarrow c \bar{u} d$  decays: the color-allowed tree diagram  $T$  (left), the color-suppressed tree diagram  $C$  (center), and the  $W$ -exchange diagram  $E$  (right). A pair of blobs denotes a four-quark operator originating through the weak interaction.

where  $A_j^0$  represents the corresponding decay amplitude without FSI. Following the procedure described in ref. [44], the scattering matrix is decomposed into a product of two matrices,  $S_{ij}^{1/2} = \sum_k (S_{\text{res}}^{1/2})_{ik} (S_2^{1/2})_{kj}$ . Then the amplitude is written as

$$\mathcal{A}_i^{\text{FSI}} = \sum_k (S_{\text{res}}^{1/2})_{ik} \mathcal{A}_k^{\text{fact}}, \quad \mathcal{A}_k^{\text{fact}} = \sum_j (S_2^{1/2})_{kj} \mathcal{A}_j^0, \quad (2.6)$$

where  $S_{\text{res}}^{1/2}$  is a rescattering matrix, and  $\mathcal{A}_k^{\text{fact}}$  is a decay amplitude which incorporates a part of FSI effects. For the color-allowed tree amplitude,  $\mathcal{A}_k^{\text{fact}}$  is assumed to correspond to the amplitude calculated in the QCDF approach.

The decay amplitude  $\mathcal{A}_k^{\text{fact}}$  can be expressed with topological amplitudes in the flavor-diagram approach based on the  $SU(3)$  flavor symmetry [14–16, 45–49]. There are three types of amplitudes for  $\bar{B}_{(s)} \rightarrow D_{(s)}^{(*)} M$  decays: the color-allowed tree amplitude  $T$ , the color-suppressed tree amplitude  $C$ , and the  $W$ -exchange amplitude  $E$ , as shown in figure 1. For example, the decay amplitude for  $B^- \rightarrow D^0 \pi^-$  is written as

$$\mathcal{A}(B^- \rightarrow D^0 \pi^-) = T_D + C_P, \quad (2.7)$$

where the subscript represents the final-state meson that involves the spectator quark. The topological amplitudes for other channels are summarized in tables 1, 2 and 3, where  $s_\phi$  and  $c_\phi$  are the sine and cosine of the mixing angle  $\phi_\eta$  in the  $\eta$ - $\eta'$  system. The definition of the mixing angle is based on ref. [50], and the single angle hypothesis  $\phi_\eta \equiv \phi_q = \phi_s$  is adopted.

In the factorization approach, the amplitudes  $T_D$  and  $C_P$  are given by

$$T_D = \frac{G_F}{\sqrt{2}} a_1(\mu) (m_B^2 - m_D^2) f_P f_0^{B \rightarrow D}(m_P^2) \quad \text{for } \bar{B} \rightarrow DP, \quad (2.8)$$

$$C_P = \frac{G_F}{\sqrt{2}} a_2(\mu) (m_B^2 - m_P^2) f_D f_0^{B \rightarrow P}(m_D^2) \quad \text{for } \bar{B} \rightarrow DP, \quad (2.9)$$

$$T_{D^*} = \frac{G_F}{\sqrt{2}} a_1(\mu) 2m_{D^*} (\epsilon^* \cdot p_B) f_P A_0^{B \rightarrow D}(m_P^2) \quad \text{for } \bar{B} \rightarrow D^* P, \quad (2.10)$$

$$C_P = \frac{G_F}{\sqrt{2}} a_2(\mu) 2m_{D^*} (\epsilon^* \cdot p_B) f_{D^*} f_+^{B \rightarrow P}(m_{D^*}^2) \quad \text{for } \bar{B} \rightarrow D^* P, \quad (2.11)$$

| Transition                | $\{S, I_z\}$  | Mode                                  | Amplitude                                 | Data                    |
|---------------------------|---------------|---------------------------------------|---|-------------------------|
| $b \rightarrow c\bar{u}d$ | $\{1, -1\}$   | $\bar{B}_s \rightarrow D_s^+ \pi^-$   | $T_D$                                     | $30.0 \pm 2.3$          |
|                           |               | $\bar{B}_s \rightarrow D^0 K^0$       | $C_P$                                     | $4.3 \pm 0.9$           |
|                           | $\{0, -3/2\}$ | $B^- \rightarrow D^0 \pi^-$           | $T_D + C_P$                               | $46.8 \pm 1.3$          |
|                           | $\{0, -1/2\}$ | $\bar{B}^0 \rightarrow D^+ \pi^-$     | $T_D + E$                                 | $25.2 \pm 1.3$          |
|                           |               | $\bar{B}^0 \rightarrow D^0 \pi^0$     | $\frac{1}{\sqrt{2}}(-C_P + E)$            | $2.63 \pm 0.14$         |
|                           |               | $\bar{B}^0 \rightarrow D^0 \eta$      | $\frac{c_\phi}{\sqrt{2}}(C_P + E)$        | $2.36 \pm 0.32$         |
|                           |               | $\bar{B}^0 \rightarrow D^0 \eta'$     | $\frac{s_\phi}{\sqrt{2}}(C_P + E)$        | $1.38 \pm 0.16$         |
|                           |               | $\bar{B}^0 \rightarrow D_s^+ K^-$     | $E$                                       | $0.27 \pm 0.05$         |
|                           | $\{-1, 0\}$   | $\bar{B}^0 \rightarrow D^+ K^-$       | $T_D$                                     | $1.86 \pm 0.20$         |
|                           |               | $\bar{B}^0 \rightarrow D^0 \bar{K}^0$ | $C_P$                                     | $0.52 \pm 0.07$         |
| $b \rightarrow c\bar{u}s$ | $\{-1, -1\}$  | $B^- \rightarrow D^0 K^-$             | $T_D + C_P$                               | $3.63 \pm 0.12$         |
|                           | $\{0, -1/2\}$ | $\bar{B}_s \rightarrow D_s^+ K^-$     | $T_D + E$                                 | $2.27 \pm 0.19^\dagger$ |
|                           |               | $\bar{B}_s \rightarrow D^0 \eta$      | $-s_\phi C_P + \frac{c_\phi}{\sqrt{2}} E$ | —                       |
|                           |               | $\bar{B}_s \rightarrow D^0 \eta'$     | $c_\phi C_P + \frac{s_\phi}{\sqrt{2}} E$  | —                       |
|                           |               | $\bar{B}_s \rightarrow D^0 \pi^0$     | $\frac{1}{\sqrt{2}} E$                    | —                       |
|                           |               | $\bar{B}_s \rightarrow D^+ \pi^-$     | $E$                                       | —                       |

**Table 1.** List of  $\bar{B} \rightarrow DP$  decays with  $b \rightarrow c\bar{u}d$  and  $b \rightarrow c\bar{u}s$  transitions. The values in the second column are the strangeness and the  $z$  component of isospin of the final state. The fourth column shows the  $SU(3)$  decomposition of the decay amplitudes. The experimental data for the CP-averaged branching ratios (in units of  $10^{-4}$ ) in the fifth column correspond to the PDG values [39], which are consistent with the HFLAV ones [51].  $^\dagger$ The data for  $\bar{B}_s \rightarrow D_s^+ K^-$  represents a sum of CP-averaged branching ratios,  $\mathcal{B}(\bar{B}_s \rightarrow D_s^+ K^-)$  and  $\mathcal{B}(\bar{B}_s \rightarrow D_s^- K^+)$ .

$$T_D = \frac{G_F}{\sqrt{2}} a_1(\mu) 2m_V(\epsilon^* \cdot p_B) f_V f_+^{B \rightarrow D}(m_V^2) \quad \text{for } \bar{B} \rightarrow DV, \quad (2.12)$$

$$C_V = \frac{G_F}{\sqrt{2}} a_2(\mu) 2m_V(\epsilon^* \cdot p_B) f_D A_0^{B \rightarrow V}(m_D^2) \quad \text{for } \bar{B} \rightarrow DV, \quad (2.13)$$

where  $\epsilon^{*\mu}$  is the polarization vector of  $D^*$  or  $V$ . The definitions of the decay constants  $f_P$ ,  $f_V$  and  $f_{D(*)}$  and the transition form factors  $f_0^{B \rightarrow D}$ ,  $f_0^{B \rightarrow P}$ ,  $f_+^{B \rightarrow P}$ ,  $f_+^{B \rightarrow D}$ ,  $A_0^{B \rightarrow D}$  and  $A_0^{B \rightarrow V}$  are found in ref. [52]. The coefficients  $a_1(\mu)$  and  $a_2(\mu)$  are evaluated at the scale  $\mu = m_b$ , where the leading-order contributions are given by  $a_1(\mu) = C_2(\mu)$  and  $a_2(\mu) = 4C_1(\mu)/9 + C_2(\mu)/3$  in terms of the Wilson coefficients in eq. (2.1).

The coefficient  $a_1(\mu)$  associated with the color-allowed tree amplitude is calculated for different processes in the framework of QCDF to the NNLO accuracy [4]:

$$a_1(m_b) = \begin{cases} (1.069_{-0.012}^{+0.009}) + (0.046_{-0.015}^{+0.023})i & \text{for } \bar{B}^0 \rightarrow D^+ K^-, \\ (1.072_{-0.013}^{+0.011}) + (0.044_{-0.014}^{+0.022})i & \text{for } \bar{B}^0 \rightarrow D^+ \pi^-, \\ (1.068_{-0.012}^{+0.010}) + (0.034_{-0.011}^{+0.017})i & \text{for } \bar{B}^0 \rightarrow D^{*+} K^-, \\ (1.071_{-0.013}^{+0.012}) + (0.032_{-0.010}^{+0.016})i & \text{for } \bar{B}^0 \rightarrow D^{*+} \pi^-. \end{cases} \quad (2.14)$$

| Transition                | $\{S, I_z\}$  | Mode                                    | Amplitude                                | Data                    |
|---------------------------|---------------|---|--|-------------------------|
| $b \rightarrow c\bar{u}d$ | $\{1, -1\}$   | $\bar{B}_s \rightarrow D_s^{*+}\pi^-$   | $T_D$                                    | $20 \pm 5$              |
|                           |               | $\bar{B}_s \rightarrow D^{*0}K^0$       | $C_P$                                    | $2.8 \pm 1.1$           |
|                           | $\{0, -3/2\}$ | $B^- \rightarrow D^{*0}\pi^-$           | $T_{D^*} + C_P$                          | $49.0 \pm 1.7$          |
|                           | $\{0, -1/2\}$ | $\bar{B}^0 \rightarrow D^{*+}\pi^-$     | $T_{D^*} + E$                            | $27.4 \pm 1.3$          |
|                           |               | $\bar{B}^0 \rightarrow D^{*0}\pi^0$     | $\frac{1}{\sqrt{2}}(-C_P + E)$           | $2.2 \pm 0.6$           |
|                           |               | $\bar{B}^0 \rightarrow D^{*0}\eta$      | $\frac{c_\phi}{\sqrt{2}}(C_P + E)$       | $2.3 \pm 0.6$           |
|                           |               | $\bar{B}^0 \rightarrow D^{*0}\eta'$     | $\frac{s_\phi}{\sqrt{2}}(C_P + E)$       | $1.40 \pm 0.22$         |
|                           |               | $\bar{B}^0 \rightarrow D_s^{*+}K^-$     | $E$                                      | $0.22 \pm 0.03$         |
|                           | $\{-1, 0\}$   | $\bar{B}^0 \rightarrow D^{*+}K^-$       | $T_{D^*}$                                | $2.12 \pm 0.15$         |
|                           |               | $\bar{B}^0 \rightarrow D^{*0}\bar{K}^0$ | $C_P$                                    | $0.36 \pm 0.12$         |
|                           | $\{-1, -1\}$  | $B^- \rightarrow D^{*0}K^-$             | $T_{D^*} + C_P$                          | $3.97^{+0.31}_{-0.28}$  |
|                           | $\{0, -1/2\}$ | $\bar{B}_s \rightarrow D_s^{*+}K^-$     | $T_{D^*} + E$                            | $1.33 \pm 0.35^\dagger$ |
|                           |               | $\bar{B}_s \rightarrow D^{*0}\eta$      | $-s_\phi C_P + \frac{c_\phi}{\sqrt{2}}E$ | —                       |
|                           |               | $\bar{B}_s \rightarrow D^{*0}\eta'$     | $c_\phi C_P + \frac{s_\phi}{\sqrt{2}}E$  | —                       |
|                           |               | $\bar{B}_s \rightarrow D^{*0}\pi^0$     | $\frac{1}{\sqrt{2}}E$                    | —                       |
|                           |               | $\bar{B}_s \rightarrow D^{*+}\pi^-$     | $E$                                      | —                       |

**Table 2.** List of  $\bar{B} \rightarrow D^*P$  decays with  $b \rightarrow c\bar{u}d$  and  $b \rightarrow c\bar{u}s$  transitions. See also the caption of table 1.  $^\dagger$ The data for  $\bar{B}_s \rightarrow D_s^{*+}K^-$  represents a sum of CP-averaged branching ratios  $\mathcal{B}(\bar{B}_s \rightarrow D_s^{*+}K^-)$  and  $\mathcal{B}(\bar{B}_s \rightarrow D_s^{*-}K^+)$ .

It is noticed that these are almost universal, and hence a common value of  $a_1(m_b)$  is used in our numerical analysis:

$$a_1(m_b) = 1.070 \pm 0.012. \quad (2.15)$$

We set  $a_1$  to be real by absorbing its phase in  $a_2$  and  $E$ , which are complex parameters in the following analysis. On the other hand, it is hard to evaluate the color-suppressed tree amplitudes reliably in QCDF, because subleading-power and non-factorizable contributions are expected to be significant. In our analysis the effective coefficient  $a_2^{\text{eff}}$  is considered to include these contributions and taken to be a free parameter. Also,  $SU(3)$  breaking effects in the amplitudes are simply assumed to be described by the factorization form as in eqs. (2.9), (2.11) and (2.13). Furthermore, the  $W$ -exchange amplitude  $E$ , which is power suppressed compared to the color-allowed amplitude  $T$ , also cannot be calculated in the QCDF approach [2]. Therefore  $E$  is taken as another free parameter under the assumption of the  $SU(3)$  flavor symmetry.

Finally, the partial decay widths for the  $b \rightarrow c\bar{u}q$  channels ( $q = d, s$ ) are expressed with the decay amplitudes as

$$\Gamma = \frac{p_{\text{cm}}}{8\pi m_B^2} |V_{cb}V_{uq}^* \mathcal{A}|^2, \quad (2.16)$$

where  $p_{\text{cm}}$  is the magnitude of the three momentum of a final-state meson in the center-of-mass frame.

| Transition                | $\{S, I_z\}$  | Mode                                     | Amplitude                      | Data            |
|---------------------------|---------------|--|--------------------------------|-----------------|
| $b \rightarrow c\bar{u}d$ | $\{1, -1\}$   | $\bar{B}_s \rightarrow D_s^+ \rho^-$     | $T_D$                          | $69 \pm 14$     |
|                           |               | $\bar{B}_s \rightarrow D^0 K^{*0}$       | $C_V$                          | $4.4 \pm 0.6$   |
|                           | $\{0, -3/2\}$ | $B^- \rightarrow D^0 \rho^-$             | $T_D + C_V$                    | $134 \pm 18$    |
|                           | $\{0, -1/2\}$ | $\bar{B}^0 \rightarrow D^+ \rho^-$       | $T_D + E$                      | $76 \pm 12$     |
|                           |               | $\bar{B}^0 \rightarrow D^0 \rho^0$       | $\frac{1}{\sqrt{2}}(-C_V + E)$ | $3.21 \pm 0.21$ |
|                           |               | $\bar{B}^0 \rightarrow D^0 \omega$       | $\frac{1}{\sqrt{2}}(C_V + E)$  | $2.54 \pm 0.16$ |
|                           |               | $\bar{B}^0 \rightarrow D^0 \phi$         | 0                              | —               |
|                           |               | $\bar{B}^0 \rightarrow D_s^+ K^{*-}$     | $E$                            | $0.35 \pm 0.10$ |
|                           |               |  |                                |                 |
| $b \rightarrow c\bar{u}s$ | $\{-1, 0\}$   | $\bar{B}^0 \rightarrow D^+ K^{*-}$       | $T_D$                          | $4.5 \pm 0.7$   |
|                           |               | $\bar{B}^0 \rightarrow D^0 \bar{K}^{*0}$ | $C_V$                          | $0.45 \pm 0.06$ |
|                           | $\{-1, -1\}$  | $B^- \rightarrow D^0 K^{*-}$             | $T_D + C_V$                    | $5.3 \pm 0.4$   |
|                           | $\{0, -1/2\}$ | $\bar{B}_s \rightarrow D_s^+ K^{*-}$     | $T_D + E$                      | —               |
|                           |               | $\bar{B}_s \rightarrow D^0 \phi$         | $-C_V$                         | $0.30 \pm 0.05$ |
|                           |               | $\bar{B}_s \rightarrow D^0 \omega$       | $\frac{1}{\sqrt{2}}E$          | —               |
|                           |               | $\bar{B}_s \rightarrow D^0 \rho^0$       | $\frac{1}{\sqrt{2}}E$          | —               |
|                           |               | $\bar{B}_s \rightarrow D^+ \rho^-$       | $E$                            | —               |
|                           |               |  |                                |                 |

**Table 3.** List of  $\bar{B} \rightarrow DV$  decays with  $b \rightarrow c\bar{u}d$  and  $b \rightarrow c\bar{u}s$  transitions. See also the caption of table 1.

## 2.2 Quasi-elastic rescattering

The framework of the quasi-elastic rescattering in  $\bar{B}_{(s)} \rightarrow D_{(s)}^{(*)}M$  was developed in refs. [27, 34, 35]. In the quasi-elastic picture, the rescattering occurs among different final states carrying the same quantum numbers. Since QCD respects the  $SU(3)$  flavor symmetry to some extent, the rescattering is considered among the states that reside in the same multiplet under the symmetry. In the case of  $\bar{B} \rightarrow DV$ , the  $U(3)$  symmetry instead of  $SU(3)$  can be applied, since there is no  $U(1)$  axial anomaly for the vector mesons. Moreover, following the procedure in ref. [44], we include a part of the  $SU(3)$  breaking effects through the meson decay constants.

Under the  $SU(3)$  flavor symmetry the  $D^{(*)}P$  final states are decomposed into one  $\bar{\mathbf{15}}$ , one  $\mathbf{6}$  and two  $\bar{\mathbf{3}}$  representations, since the light pseudo-scalar mesons transform as  $\mathbf{8}$  and  $\mathbf{1}$ , and the charm mesons  $D^{(*)0}$ ,  $D^{(*)+}$  and  $D_s^{(*)+}$  form a  $\bar{\mathbf{3}}$  representation. Therefore, the rescattering matrix in eq. (2.6) can be written in the  $SU(3)$  basis as [27]

$$S_{\text{res}}^{1/2} = e^{i\delta_{\bar{\mathbf{15}}}} \sum_{a=1}^{15} |\bar{\mathbf{15}}; a\rangle \langle \bar{\mathbf{15}}; a| + e^{i\delta_{\mathbf{6}}} \sum_{b=1}^6 |\mathbf{6}; b\rangle \langle \mathbf{6}; b| + \sum_{m,n=\bar{\mathbf{3}}, \bar{\mathbf{3}}'}^3 |m; c\rangle \mathcal{U}_{mn}^{1/2} \langle n; c|, \quad (2.17)$$

where  $\mathcal{U}^{1/2}$  is a  $2 \times 2$  symmetric unitary matrix. Since the overall phase is not physical, the phase difference,

$$\delta' \equiv \delta_{\mathbf{6}} - \delta_{\bar{\mathbf{15}}}, \quad (2.18)$$



is defined, and  $\mathcal{U}^{1/2}$  is parameterized in terms of three parameters  $\theta$ ,  $\sigma$  and  $\tau$  (see, e.g., ref. [36]):

$$\mathcal{U}'_{mn} \equiv \mathcal{U}^{1/2} e^{-i\delta_{15}} = \begin{pmatrix} \cos \tau & \sin \tau \\ -\sin \tau & \cos \tau \end{pmatrix} \begin{pmatrix} e^{i\theta} & 0 \\ 0 & e^{i\sigma} \end{pmatrix} \begin{pmatrix} \cos \tau & -\sin \tau \\ \sin \tau & \cos \tau \end{pmatrix}. \quad (2.19)$$

Thus the rescattering matrix is parameterized by the four parameters  $\delta'$ ,  $\theta$ ,  $\sigma$  and  $\tau$ . Note that the rescattering effects are turned off at  $\delta' = \theta = \sigma = \tau = 0$ .

The rescattering in the  $D^{(*)}V$  final states can be parameterized in a similar way. The light vector mesons form a  $U(3)$  nonet instead of a  $SU(3)$  octet. In this case the rescattering parameters have specific values as follows, which are called “solution 1” and “solution 2” in ref. [27]:

$$\bullet \text{ Solution 1 : } \delta' = \theta, \quad \sigma = 0, \quad \sin \tau = \sqrt{\frac{1}{3}}, \quad \cos \tau = \sqrt{\frac{2}{3}}, \quad (2.20)$$

$$\bullet \text{ Solution 2 : } \delta' = \theta = 0, \quad \sin \tau = \frac{2\sqrt{2}}{3}, \quad \cos \tau = \frac{1}{3}. \quad (2.21)$$

Hence only a single parameter is left free for each solution.

In the following the rescattering formulae are presented for the  $\bar{B} \rightarrow DP$  decays. The corresponding formulae for  $\bar{B} \rightarrow D^*P$  and  $\bar{B} \rightarrow DV$  can be obtained by substituting the final-state mesons appropriately.

The final states are classified by the strangeness and the isospin. There are three sets for the decays with the  $b \rightarrow c\bar{u}d$  transition:  $\{S, I_z\} = \{0, -3/2\}$ ,  $\{0, -1/2\}$  and  $\{1, -1\}$ . For  $\bar{B} \rightarrow DP$ ,  $\{S, I_z\} = \{0, -3/2\}$  corresponds only to the single process  $\bar{B} \rightarrow D^0\pi^-$ . Then the elastic rescattering causes only an unphysical overall phase shift, and thus, does not alter the branching ratio of this channel. For the other sets the decay amplitudes are assembled as

$$\mathcal{A}_{d,0,-1/2} = \begin{pmatrix} \mathcal{A}(\bar{B}^0 \rightarrow D^+\pi^-) \\ \mathcal{A}(\bar{B}^0 \rightarrow D^0\pi^0) \\ \mathcal{A}(\bar{B}^0 \rightarrow D_s^+K^-) \\ \mathcal{A}(\bar{B}^0 \rightarrow D^0\eta_8) \\ \mathcal{A}(\bar{B}^0 \rightarrow D^0\eta_1) \end{pmatrix}, \quad \mathcal{A}_{d,1,-1} = \begin{pmatrix} \mathcal{A}(\bar{B}_s \rightarrow D_s^+\pi^-) \\ \mathcal{A}(\bar{B}_s \rightarrow D^0K^0) \end{pmatrix}, \quad (2.22)$$

where the subscripts denote the flavor of the down-type quark, the strangeness and the isospin of the final states. The physical states,  $\eta$  and  $\eta'$ , are given in terms of the octet state  $\eta_8$  and the singlet one  $\eta_1$  as  $\eta = \eta_8 \cos \theta_\eta - \eta_1 \sin \theta_\eta$  and  $\eta' = \eta_8 \sin \theta_\eta + \eta_1 \cos \theta_\eta$  with  $\theta_\eta = \phi_\eta - \arctan \sqrt{2}$ .

Similarly, the final states in the processes with the  $b \rightarrow c\bar{u}s$  transition are classified into  $\{S, I_z\} = \{-1, -1\}$ ,  $\{-1, 0\}$  and  $\{0, -1/2\}$ . For  $\{S, I_z\} = \{-1, -1\}$ , there is only the

single process  $B^- \rightarrow D^0 K^-$ . The decay amplitudes for the others are written as

$$\mathcal{A}_{s,-1,0} = \begin{pmatrix} \mathcal{A}(\bar{B}^0 \rightarrow D^+ K^-) \\ \mathcal{A}(\bar{B}^0 \rightarrow D^0 \bar{K}^0) \end{pmatrix}, \quad \mathcal{A}_{s,0,-1/2} = \begin{pmatrix} \mathcal{A}(\bar{B}_s \rightarrow D^+ \pi^-) \\ \mathcal{A}(\bar{B}_s \rightarrow D^0 \pi^0) \\ \mathcal{A}(\bar{B}_s \rightarrow D_s^+ K^-) \\ \mathcal{A}(\bar{B}_s \rightarrow D^0 \eta_8) \\ \mathcal{A}(\bar{B}_s \rightarrow D^0 \eta_1) \end{pmatrix}. \quad (2.23)$$

According to eq. (2.6), the rescattering is incorporated into the decay amplitudes as

$$\mathcal{A}_{q,S,I_z}^{\text{FSI}} = V_{S,I_z}^{-1} \mathcal{S}_{S,I_z}^{1/2} V_{S,I_z} \mathcal{A}_{q,S,I_z}^{\text{fact}}, \quad (2.24)$$

where  $\mathcal{S}_{0,-1/2}^{1/2}$  is the rescattering matrix, and the matrix  $V_{S,I_z}$  represents the  $SU(3)$  breaking effects [44]. It is noticed that the breaking effects are removed from  $\mathcal{A}_{q,S,I_z}^{\text{fact}}$  before the rescattering by applying  $V_{S,I_z}$ , and then put them back after the rescattering by  $V_{S,I_z}^{-1}$  [44], since the rescattering is considered to work under the  $SU(3)$  symmetry.

The explicit expressions of the symmetric matrices  $\mathcal{S}_{S,I_z}^{1/2}$  are given by [27, 34, 35]

$$\mathcal{S}_{1,-1}^{1/2} = \mathcal{S}_{-1,0}^{1/2} = \frac{e^{i\delta_{1\bar{5}}}}{2} \begin{pmatrix} 1 + e^{i\delta'} & 1 - e^{i\delta'} \\ 1 + e^{i\delta'} \end{pmatrix}, \quad (2.25)$$

$$\mathcal{S}_{0,-1/2}^{1/2} = \frac{e^{i\delta_{1\bar{5}}}}{8} \begin{pmatrix} 3 + u_+ & -\frac{1}{\sqrt{2}}(5 - u_+) & -1 - u_- & \sqrt{\frac{3}{2}}(1 - v_-) & \sqrt{6}u' \\ & \frac{1}{2}(11 + u_+) & -\frac{1}{\sqrt{2}}(1 + u_-) & \frac{\sqrt{3}}{2}(1 - v_-) & \sqrt{3}u' \\ & & 3 + u_+ & -\sqrt{\frac{3}{2}}(3 - v_+) & \sqrt{6}u' \\ & & & \frac{1}{2}(9 + w_+) & u' \\ & & & & u'' \end{pmatrix}, \quad (2.26)$$

where  $u_{\pm} = 2e^{i\delta'} \pm 3\mathcal{U}'_{\bar{3}\bar{3}}$ ,  $v_{\pm} = 2e^{i\delta'} \pm \mathcal{U}'_{\bar{3}\bar{3}}$ ,  $w_+ = 6e^{i\delta'} + \mathcal{U}'_{\bar{3}\bar{3}}$ ,  $u' = 2\mathcal{U}'_{\bar{3}\bar{3}}$ , and  $u'' = 8\mathcal{U}'_{\bar{3}'\bar{3}'}$ , and the lower components are omitted for simplicity. The matrix  $V_{-1,0}$  is a unit matrix, and the others are modeled by the ratios of the meson decay constants (see ref. [44]):

$$V_{1,-1} = \text{diag}\left(1, \frac{f_{D_s} f_{\pi}}{f_D f_K}\right), \quad (2.27)$$

$$V_{0,-1/2} = \text{diag}\left(1, 1, \frac{f_D f_{\pi}}{f_{D_s} f_K}, \frac{f_D f_{\pi}}{f_D f_{\eta_8}}, \frac{f_D f_{\pi}}{f_D f_{\eta_1}}\right). \quad (2.28)$$

For the  $\bar{B} \rightarrow DV$  decays with  $\{S, I_z\} = \{0, -1/2\}$ , we calculate the amplitudes  $\mathcal{A}_{q,0,-1/2}^{\text{fact}}$  in the basis with  $\phi$  and  $\omega$  instead of the  $SU(3)$  states:

$$\mathcal{A}_{d,0,-1/2} = \begin{pmatrix} \mathcal{A}(\bar{B}^0 \rightarrow D^+ \rho^-) \\ \mathcal{A}(\bar{B}^0 \rightarrow D^0 \rho^0) \\ \mathcal{A}(\bar{B}^0 \rightarrow D_s^+ K^{*-}) \\ \mathcal{A}(\bar{B}^0 \rightarrow D^0 \phi) \\ \mathcal{A}(\bar{B}^0 \rightarrow D^0 \omega) \end{pmatrix}, \quad \mathcal{A}_{s,0,-1/2} = \begin{pmatrix} \mathcal{A}(\bar{B}_s \rightarrow D^+ \rho^-) \\ \mathcal{A}(\bar{B}_s \rightarrow D^0 \rho^0) \\ \mathcal{A}(\bar{B}_s \rightarrow D_s^+ K^{*-}) \\ \mathcal{A}(\bar{B}_s \rightarrow D^0 \phi) \\ \mathcal{A}(\bar{B}_s \rightarrow D^0 \omega) \end{pmatrix}. \quad (2.29)$$

In this case the rescattering formula includes the mixing of the states as

$$\mathcal{A}_{q,0,-1/2}^{\text{FSI}} = (V_{0,-1/2}^{DV})^{-1} (U^{DV})^\dagger \mathcal{S}_{0,-1/2}^{1/2} U^{DV} V_{0,-1/2}^{DV} \mathcal{A}_{q,0,-1/2}^{\text{fact}}, \quad (2.30)$$

where  $U^{DV}$  and  $V_2^{DV}$  are defined by

$$U^{DV} = \begin{pmatrix} 1 & 0 & 0 & 0 & 0 \\ 0 & 1 & 0 & 0 & 0 \\ 0 & 0 & 1 & 0 & 0 \\ 0 & 0 & 0 & \cos \theta_V & \sin \theta_V \\ 0 & 0 & 0 & -\sin \theta_V & \cos \theta_V \end{pmatrix}, \quad (2.31)$$

$$V_{0,-1/2}^{DV} = \text{diag} \left( 1, 1, \frac{f_D f_\rho}{f_{D_s} f_{K^*}}, \frac{f_D f_\rho}{f_D f_\phi}, \frac{f_D f_\rho}{f_D f_\omega} \right). \quad (2.32)$$

The angle  $\theta_V$  represents the mixing of the octet and singlet states:  $\phi = \omega_8 \cos \theta_V - \omega_1 \sin \theta_V$  and  $\omega = \omega_8 \sin \theta_V + \omega_1 \cos \theta_V$  with  $\cos \theta_V = \sqrt{2/3}$  and  $\sin \theta_V = 1/\sqrt{3}$ .

### 3 Numerical analysis

The input parameters for our numerical analysis are summarized in table 4. The decay constants and the mixing angle for the octet and singlet states of the pseudo-scalar mesons are chosen as  $f_8 = 1.27 f_\pi$ ,  $f_1 = 1.14 f_\pi$ , and  $\theta_\eta = \phi_\eta - \arctan \sqrt{2}$  with  $\phi_\eta = 0.7036$  rad [50]. Other parameters, such as the Fermi constant  $G_F$  and the masses and the lifetimes of the mesons, are taken from ref. [39]. Note that the value of  $V_{cb}$  in this section corresponds to the so-called exclusive  $V_{cb}$ . If the inclusive  $V_{cb}$ , which is larger than the exclusive one by about 5% [39], is used, the tensions between the experimental data and the theoretical predictions for the color-allowed decays are enhanced.

#### 3.1 Color-allowed decays

As pointed out in ref. [5], the theoretical predictions for the branching ratios of the color-allowed  $\bar{B} \rightarrow DP$  and  $\bar{B} \rightarrow D^*P$  decays are universally larger than the measured values. Let us first update the predictions in ref. [5] by adopting the latest results of the  $\bar{B} \rightarrow D^{(*)}$  form factors given in ref. [37]. The  $\bar{B} \rightarrow D^*$  form factors in ref. [37] have smaller uncertainties compared to those in ref. [6] because they include the full distribution data reported from Belle [60, 61] and QCD sum rule constraints on the parameters appearing in higher order corrections. It is assumed that the values of the  $\bar{B}_s \rightarrow D_s^{(*)}$  form factors are identical to those of the  $\bar{B} \rightarrow D^{(*)}$  form factors, because the  $SU(3)$  breaking effects between them are found to be insignificant [6, 38]. Then, ignoring the rescattering contributions, the following predictions are obtained for the CP-averaged branching ratios of the color-allowed tree channels:

$$\mathcal{B}(\bar{B}_s \rightarrow D_s^+ \pi^-) = (40.9 \pm 2.1) \times 10^{-4}, \quad (3.1)$$

$$\mathcal{B}(\bar{B}^0 \rightarrow D^+ K^-) = (3.03 \pm 0.15) \times 10^{-4}, \quad (3.2)$$

$$\mathcal{B}(\bar{B}_s \rightarrow D_s^{*+} \pi^-) = (44.6 \pm 2.2) \times 10^{-4}, \quad (3.3)$$

| Parameter                    | Value          | Parameter                | Value          | Parameter                   | Value          |
|------------------------------|----------------|--------------------------|----------------|-----------------------------|----------------|
| $ V_{ud} $                   | 0.97370 [39]   | $ V_{us} $               | 0.2245 [39]    | $ V_{cb} $                  | 0.0397(6) [37] |
| $f_D$                        | 0.2127 [53]    | $f_\pi$                  | 0.1302(8) [54] | $f_K$                       | 0.1557(3) [54] |
| $f_{D_s}$                    | 0.2499 [53]    | $f_\rho$                 | 0.213(5) [55]  | $f_{K^*}$                   | 0.204(7) [55]  |
| $f_{D^*}$                    | 0.249 [52]     | $f_\phi$                 | 0.233(4) [55]  | $f_\omega$                  | 0.197(8) [55]  |
| $f_{D_s^*}$                  | 0.293 [56]     |                          |                |                             |                |
| $F_0^{BD}(m_\pi^2)$          | 0.669(10) [37] | $F_0^{BD}(m_K^2)$        | 0.672(10) [37] | $F_1^{BD}(m_\rho^2)$        | 0.686(10) [37] |
| $F_1^{BD}(m_{K^*}^2)$        | 0.692(10) [37] |                          |                |                             |                |
| $A_0^{BD^*}(m_\pi^2)$        | 0.725(14) [37] | $A_0^{BD^*}(m_K^2)$      | 0.732(14) [37] | $A_0^{BD^*}(m_\eta^2)$      | 0.734(14) [37] |
| $A_0^{BD^*}(m_{\eta'}^2)$    | 0.754(14) [37] |                          |                |                             |                |
| $F_0^{B\pi}(m_D^2)$          | 0.288 [57]     | $F_0^{BK}(m_D^2)$        | 0.364 [57]     | $F_0^{B\eta}(m_D^2)$        | 0.192 [58]     |
| $F_0^{B\eta'}(m_D^2)$        | 0.148 [58]     | $F_0^{B_s K}(m_D^2)$     | 0.310 [57, 59] | $F_0^{B_s \eta}(m_D^2)$     | -0.243 [58]    |
| $F_0^{B_s \eta'}(m_D^2)$     | 0.290 [58]     |                          |                |                             |                |
| $F_1^{B\pi}(m_{D^*}^2)$      | 0.328 [57]     | $F_1^{BK}(m_{D^*}^2)$    | 0.420 [57]     | $F_1^{B\eta}(m_{D^*}^2)$    | 0.210 [58]     |
| $F_1^{B\eta'}(m_{D^*}^2)$    | 0.162 [58]     | $F_1^{B_s K}(m_{D^*}^2)$ | 0.357 [57, 59] | $F_1^{B_s \eta}(m_{D^*}^2)$ | -0.264 [58]    |
| $F_1^{B_s \eta'}(m_{D^*}^2)$ | 0.311 [58]     |                          |                |                             |                |
| $A_0^{B\rho}(m_D^2)$         | 0.432 [55]     | $A_0^{B\omega}(m_D^2)$   | 0.399 [55]     | $A_0^{BK^*}(m_D^2)$         | 0.458 [55]     |
| $A_0^{B_s K^*}(m_D^2)$       | 0.438 [55]     | $A_0^{B_s \phi}(m_D^2)$  | 0.515 [55]     |                             |                |

**Table 4.** The CKM matrix elements, decay constants in units of GeV,  $\bar{B} \rightarrow D^{(*)}$  form factors,  $\bar{B}_{(s)} \rightarrow P$  form factors, and  $\bar{B}_{(s)} \rightarrow V$  form factors. The definitions of the  $\bar{B}_{(s)} \rightarrow \eta^{(\prime)}$  form factors include the mixing angle and the Clebsch-Gordan coefficients. We assume that the values of the  $\bar{B}_s \rightarrow D_s^{(*)}$  form factors are identical to those of the  $\bar{B} \rightarrow D^{(*)}$  form factors [6, 38].

$$\mathcal{B}(\bar{B}^0 \rightarrow D^{*+} K^-) = (3.27 \pm 0.16) \times 10^{-4}, \quad (3.4)$$

$$\mathcal{B}(\bar{B}_s \rightarrow D_s^+ \rho^-) = (104.5 \pm 7.1) \times 10^{-4}, \quad (3.5)$$

$$\mathcal{B}(\bar{B}^0 \rightarrow D^+ K^{*-}) = (4.91 \pm 0.41) \times 10^{-4}. \quad (3.6)$$

The uncertainties come mainly from  $|V_{cb}|$ ,  $f_{P(V)}$  and the  $B_{(s)} \rightarrow D_{(s)}^{(*)}$  form factors in table 4 as well as from  $a_1$  in eq. (2.15), where the correlations between  $|V_{cb}|$  and the  $B_{(s)} \rightarrow D_{(s)}^{(*)}$  form factors are included. The combined uncertainties are at the level of 5% for  $\bar{B} \rightarrow DP$  and  $\bar{B} \rightarrow D^*P$  and of 7 to 8% for  $\bar{B} \rightarrow DV$ . It is found that the predicted branching ratios for  $\bar{B}_s \rightarrow D_s^+ \pi^-$  and  $\bar{B}^0 \rightarrow D^+ K^-$  become slightly larger than the previous results in Ref. [5]. Also the uncertainty in  $\bar{B} \rightarrow D^*P$  is smaller due to the update of the form factors in Ref. [37]. Consequently, the above results deviate from the measured values by  $3.5\sigma$ ,  $4.7\sigma$ ,  $4.5\sigma$ ,  $5.3\sigma$ ,  $2.3\sigma$  and  $0.5\sigma$ , respectively. It is noted that the discrepancies are milder in the case of  $\bar{B} \rightarrow DV$ . Especially, the prediction for  $\mathcal{B}(\bar{B}^0 \rightarrow D^+ K^{*-})$  is consistent with the data.

The above predictions are very clean theoretically. There is neither penguin nor annihilation contribution to these processes. As a result, there is no chirally-enhanced hard-scattering contributions at  $\mathcal{O}(\Lambda_{\text{QCD}}/m_B)$ . Moreover, power corrections at  $\mathcal{O}(\Lambda_{\text{QCD}}/m_B)$ , including twist-3 two-particle contributions of light-meson light-cone distribution ampli-

tudes, a hard-collinear gluon exchange between  $b$  (or  $c$ ) and the light meson, and a soft gluon exchange between the  $B \rightarrow D$  system and the light meson, are expected to be less than a percent [5]. Besides, the QCD $\times$ QED factorization is studied recently in ref. [62], where QED contributions to the color-allowed tree amplitudes are found to reduce the total amplitudes by the sub-percent level, though ultrasoft photons may correct the measured decay rates up to a few percent.

### 3.2 Rescattering between color-allowed and color-suppressed decays

The rescattering effects modify the predictions for the color-allowed tree channels. In this subsection we investigate whether the quasi-elastic rescattering contributions based on the  $SU(3)$  and  $U(3)$  flavor symmetries can explain the discrepancies between the theoretical prediction and the experimental data discussed in the last subsection.

As explained in section 2.2, the color-allowed tree decay  $\bar{B}_s \rightarrow D_s^+ \pi^-$  receives the quasi-elastic rescattering through the process  $\bar{B}_s \rightarrow D^0 K^0 \rightarrow D_s^+ \pi^-$ , where  $\bar{B}_s \rightarrow D^0 K^0$  is a color-suppressed tree decay. The correlations between the color-allowed and the color-suppressed decays are shown in figure 2. Here the color-suppressed tree amplitude is parameterized with a single complex parameter  $a_2^{\text{eff}}$ , which is substituted for  $a_2(\mu)$  in eqs. (2.9), (2.11) and (2.13) and includes the factorizable and non-factorizable contributions. Then,  $|a_2^{\text{eff}}|$  and  $\arg(a_2^{\text{eff}})$  are taken as free parameters. Also, the rescattering contributions are parameterized by a single parameter  $\delta'$  as in eq. (2.25). In the numerical analyses, the CP-conserving strong phase  $\arg(a_2^{\text{eff}})$  and the rescattering phase  $\delta'$  are scanned from 0 to  $2\pi$ . In particular, for  $\bar{B} \rightarrow DV$ , the solution 1 in eq. (2.20) is adopted because  $\delta' = 0$  is set in the solution 2. The uncertainties of the input parameters in table 4 are ignored here.

In figure 2, the solid black lines denote the contours for  $|a_2^{\text{eff}}| = 0.0, 0.2, 0.4, 0.6$  and  $0.8$ . For example, in the case of  $\bar{B}_s \rightarrow D_s^+ \pi^-$  and  $\bar{B}_s \rightarrow D^0 K^0$ , the branching ratios satisfy the following relation:

$$\frac{\mathcal{B}(\bar{B}_s \rightarrow D^0 K^0) - \mathcal{B}(\bar{B}_s \rightarrow D^0 K^0)|_{\delta'=0}}{\mathcal{B}(\bar{B}_s \rightarrow D_s^+ \pi^-) - \mathcal{B}(\bar{B}_s \rightarrow D_s^+ \pi^-)|_{\delta'=0}} = -\frac{p_{\text{cm}, D^0 K^0}}{p_{\text{cm}, D_s^+ \pi^-}} \left( \frac{f_D f_K}{f_{D_s} f_\pi} \right)^2, \quad (3.7)$$

where  $p_{\text{cm}, D_s^+ \pi^-}$  and  $p_{\text{cm}, D^0 K^0}$  are the magnitude of the three momentum of a final-state meson in the center-of-mass frame in each process. If the rescattering contribution is absent, there are tensions between the theoretical predictions (denoted by a red dotted line) and the experimental data (denoted by yellow vertical bands) for the color-allowed tree decay. Their branching ratios can be reduced by including the rescattering contribution, while the ratios for the color-suppressed channels increase at the same time. Although smaller  $|a_2^{\text{eff}}|$  is preferred from the data, even with  $|a_2^{\text{eff}}| = 0.0$ , there still remain a discrepancy between the theoretical results and the experimental data for  $\bar{B} \rightarrow D^{(*)}P$ . Therefore, we conclude that the experimental data cannot be fully explained even if the quasi-elastic rescattering contributions are included.

The discrepancy may be explained by introducing rescattering contributions beyond the quasi-elastic approximation, large power corrections in the QCDF approach and/or NP contributions. Here the latter two cases are studied by regarding the coefficient  $a_1(m_b)$  as an additional free parameter. In figure 3 the region of  $a_1(m_b)$  and  $|a_2^{\text{eff}}|$  that accommodate

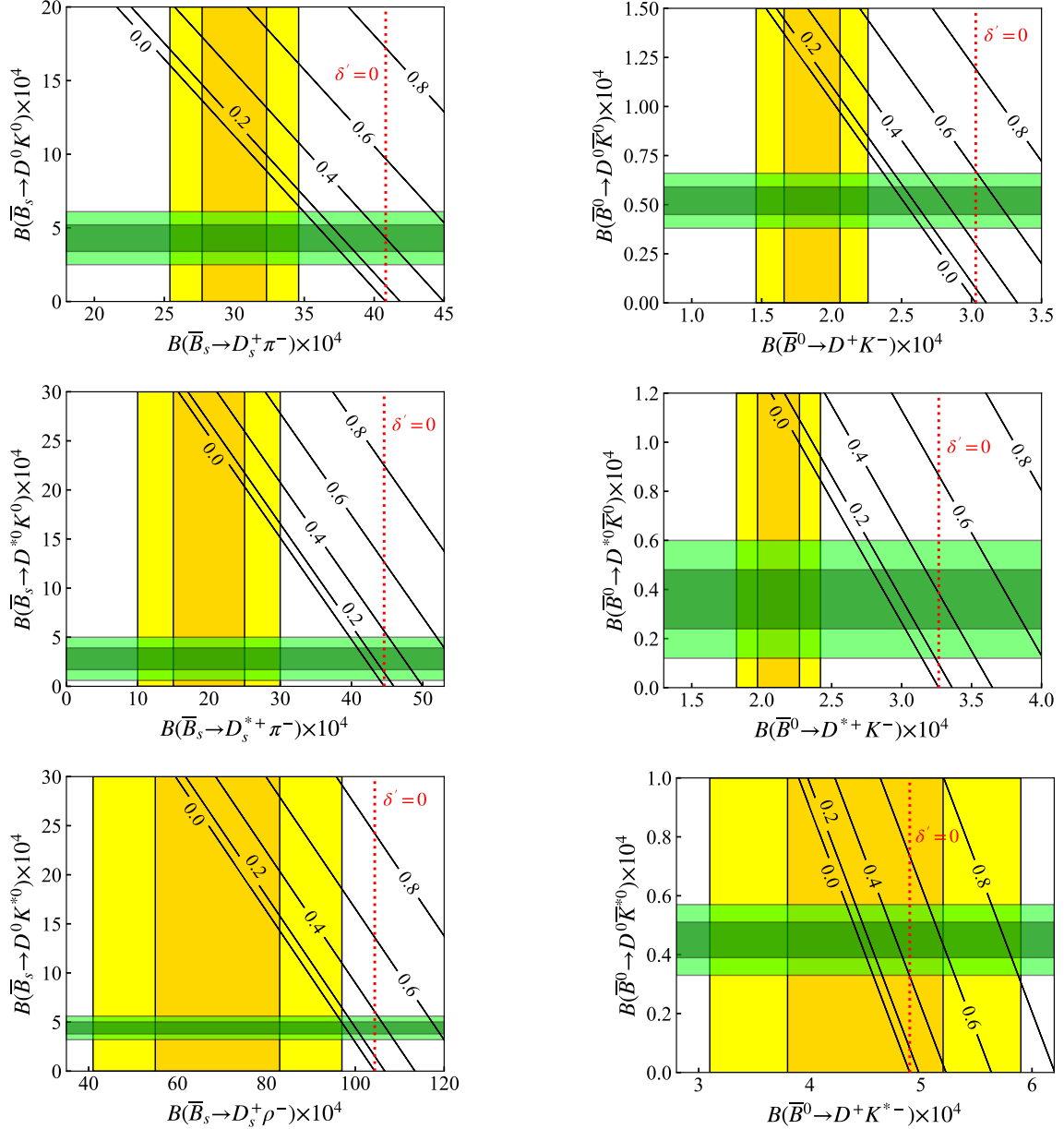


**Figure 2.** Contours of the effective coefficient  $|a_2^{\text{eff}}|$  for the color-suppressed tree amplitude in the plane of the branching ratios for the color-allowed-tree and color-suppressed-tree channels, where the rescattering phase  $\delta'$  and the relative phase between  $a_1(m_b)$  and  $a_2^{\text{eff}}$  are taken to be free. The vertical (yellow) and horizontal (green) bands show the experimental constraints on the branching ratios at the  $1\sigma$  (darker) and  $2\sigma$  (lighter) levels. The vertical dotted line (red) corresponds to the case of no rescattering, i.e.,  $\delta' = 0$ .

the experimental data for the color-allowed and color-suppressed channels simultaneously is presented. For example, the colored regions in the top-left plot are calculated with the relation,

$$\alpha r |a_1(m_b)|^2 + \beta |a_2^{\text{eff}}|^2 = r \mathcal{B}(\bar{B}_s \rightarrow D_s^+ \pi^-) + \mathcal{B}(\bar{B}_s \rightarrow D^0 K^0), \quad (3.8)$$

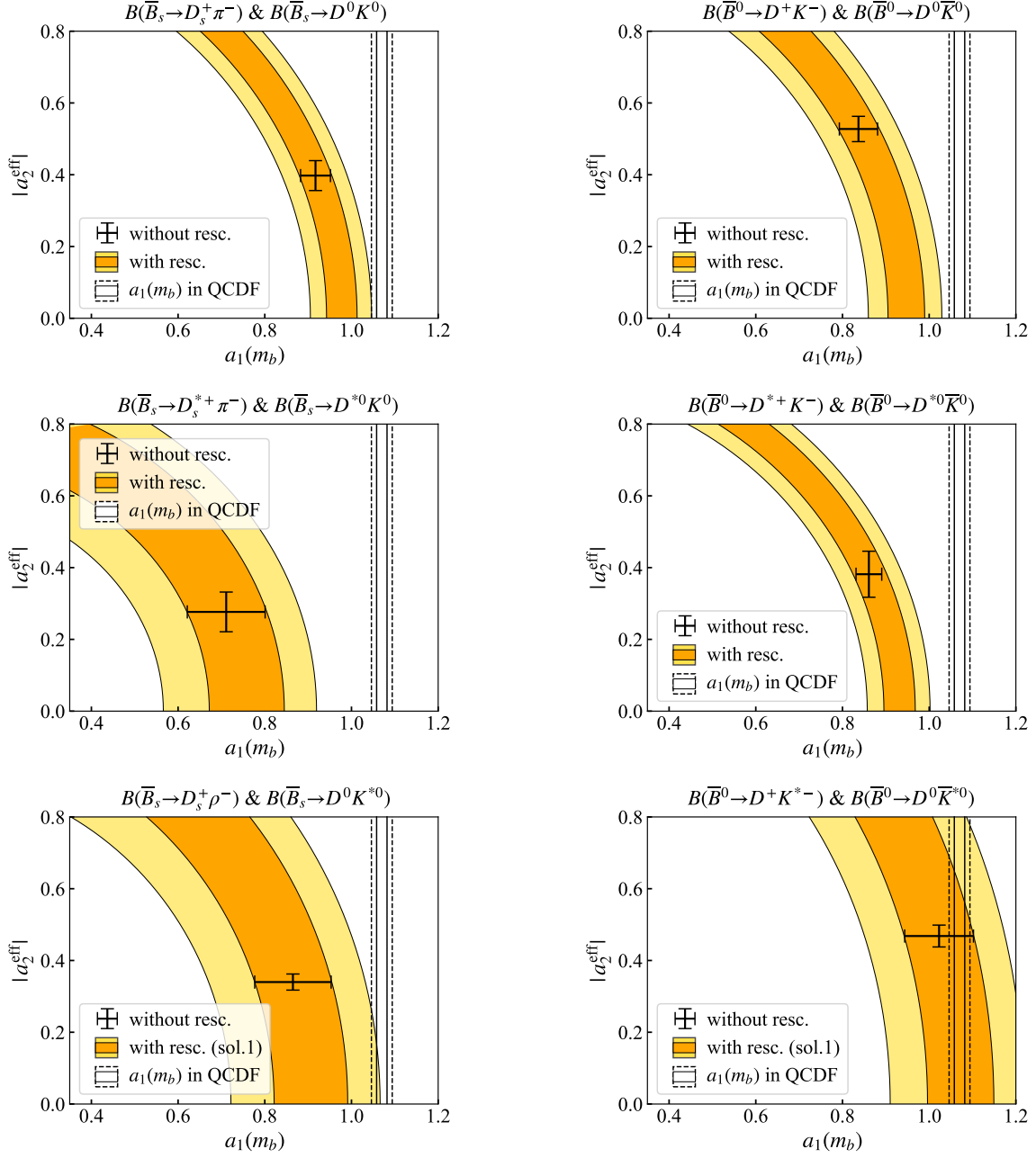


**Figure 3.** The favored region in  $a_1(m_b)$  vs  $|a_2^{\text{eff}}|$  plane considering color-allowed and color-suppressed channels simultaneously. The orange regions show the experimental constraints at  $1\sigma$  (darker) and  $2\sigma$  (lighter) levels including the rescattering. The cross in the band shows the result calculated without the rescattering. Black solid and dashed bands correspond to the QCDF prediction at the  $1\sigma$  and  $2\sigma$  levels.

where  $r = (p_{\text{cm}, D^0 K^0} / p_{\text{cm}, D_s^+ \pi^-}) (f_D f_K / f_{D_s} f_\pi)^2$ ,  $\alpha = \mathcal{B}(\overline{B}_s \rightarrow D_s^+ \pi^-)|_{a_1(m_b)=1, \delta'=0}$  and  $\beta = \mathcal{B}(\overline{B}_s \rightarrow D^0 K^0)|_{a_2^{\text{eff}}=1, \delta'=0}$ . The orange regions show the experimental constraints on the branching ratios at the  $1\sigma$  (darker) and  $2\sigma$  (lighter) levels, where  $\arg(a_2^{\text{eff}})$  and  $\delta'$  are

scanned from 0 to  $2\pi$ . Here and hereafter, new CP-violating phases are assumed to be absent for simplicity. It is observed that universal downward shifts of  $\mathcal{O}(10\%)$  in  $a_1(m_b)$  improve the overall consistency between the theoretical and experimental results. It is noted that the values of  $|a_2^{\text{eff}}|$  from each channel can be different from each other due to differences in the non-factorizable contributions among  $\bar{B} \rightarrow DP$ ,  $\bar{B} \rightarrow D^*P$  and  $\bar{B} \rightarrow DV$  as well as to the  $SU(3)$  breaking effects.

When the rescattering effects are neglected, one can determine  $a_1(m_b)$  and  $|a_2^{\text{eff}}|$  individually from the branching ratios for the color-allowed and color-suppressed channels, respectively. The result is denoted by the cross in the figure. It is found that there are mild tensions among the values of  $a_1(m_b)$  determined from each channel. However, these tensions can be reduced by including the quasi-elastic rescattering.

### 3.3 Global analysis

As shown in the last subsection, the shift of  $a_1(m_b)$  away from the QCDF prediction depends on the values of  $|a_2^{\text{eff}}|$ ,  $\arg(a_2^{\text{eff}})$  and  $\delta'$ . The other decay channels listed in tables 1, 2 and 3 provide constraints on these parameters under the  $SU(3)$  and  $U(3)$  flavor symmetries. In particular, the decays with the amplitude  $T + C$ , such as  $B^- \rightarrow D^0\pi^-$ , give an information on correlations among  $a_1(m_b)$ ,  $|a_2^{\text{eff}}|$  and  $\arg(a_2^{\text{eff}})$ . It is noted that they do not receive rescattering contribution.

In the analysis, the global-fitting package `HEPfit` [63] is used with our own implementation of the  $\bar{B}_{(s)} \rightarrow D_{(s)}^{(*)}M$  observables to investigate the constraints from the available data. The statistical analysis of the package is based on the `BAT` library [64], which allows us to evaluate the posterior probability distributions of the parameters based on the Bayesian statistical inference with the Markov Chain Monte Carlo (MCMC).

The following two cases are considered: (i) a fit with only the six decay modes that have the amplitude  $T$ ,  $C$  or  $T + C$ , and (ii) a fit with all the modes for which the experimental data are available. The four parameters  $a_1(m_b)$ ,  $\text{Re}(a_2^{\text{eff}})$ ,  $\text{Im}(a_2^{\text{eff}})$  and  $\delta'$  are floated in the former case, while the nine parameters  $a_1(m_b)$ ,  $\text{Re}(a_2^{\text{eff}})$ ,  $\text{Im}(a_2^{\text{eff}})$ ,  $\text{Re}(E)$ ,  $\text{Im}(E)$ ,  $\delta'$ ,  $\theta$ ,  $\sigma$  and  $\tau$  are floated in the latter. Flat priors are assumed for the fit parameters. Other parameters are fixed to be constant in the fits. The experimental constraints are listed in tables 1, 2 and 3.<sup>10</sup> The data for  $\mathcal{B}(\bar{B}_s \rightarrow D_s^{(*)+}K^-)$  are not included in the fits, because they are the sum of the branching ratios of  $b \rightarrow c\bar{u}s$  and  $b \rightarrow u\bar{c}s$  transitions. The branching ratio for  $\bar{B}_s \rightarrow D_s^{(*)-}K^+$  is expected to be of the same order of magnitude as that for  $\bar{B}_s \rightarrow D_s^{(*)+}K^-$ . In figure 4 the two-dimensional probability distributions of  $a_1(m_b)$  and  $|a_2^{\text{eff}}|$  are presented for the fit (i) in the left plots and for the fit (ii) in the right plots. The solution 1 in eq. (2.20) is adopted for  $\bar{B} \rightarrow DV$ . The results for the solution 2 in eq. (2.21), which are not presented in figure 4, become similar to those for the solution 1 without the rescattering, since the rescattering parameter  $\delta'$  is fixed to zero. In each plot, the blue (red) region shows the fit result with (without) the rescattering. Here and in the following figures the darker (lighter) region corresponds to the 68% (95%) probability. By comparing the left plots in figure 4 with the plots in figure 3, it is found that the preferred

<sup>10</sup>A recent data  $\mathcal{B}(B^- \rightarrow D^{*0}\pi^-) = (53.5 \pm 2.2) \times 10^{-4}$  from LHCb [65] is not included.



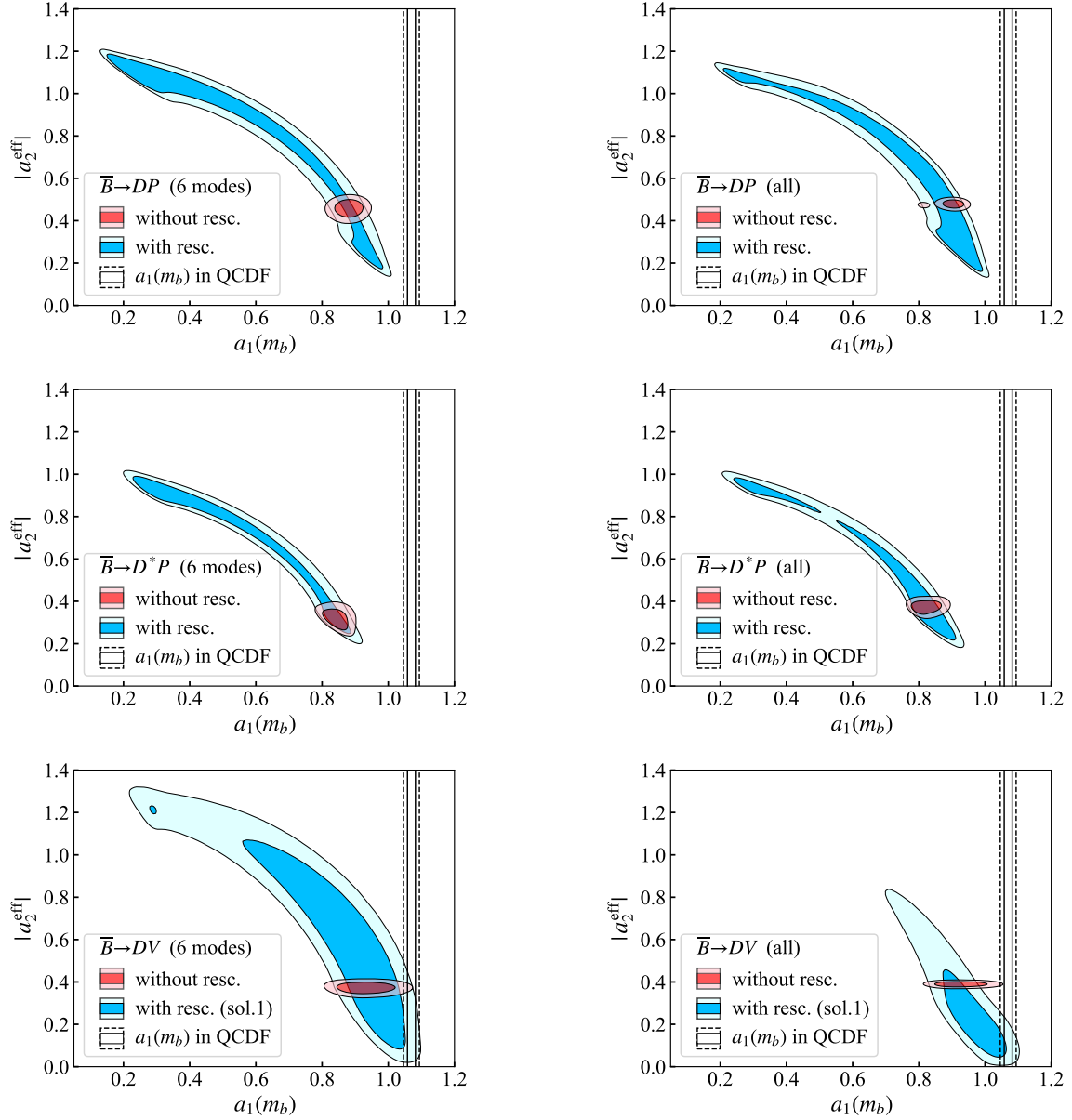


**Figure 4.** Two-dimensional probability distributions of  $a_1(m_b)$  and  $|a_2^{\text{eff}}|$ . The darker (lighter) regions correspond to the 68% (95%) probability. For the rescattering parameters in  $\bar{B} \rightarrow DV$ , the solution 1 is adopted.

regions are diminished partly by including the  $T + C$  modes. The regions in the right plots are basically similar to those in the left plots except for those of  $\bar{B} \rightarrow DV$ . Thus, the fit is not improved even if the decay modes with the exchange amplitude  $E$  are included, because the additional five fit parameters  $\text{Re}(E)$ ,  $\text{Im}(E)$ ,  $\theta$ ,  $\sigma$  and  $\tau$  are introduced in the fit of  $\bar{B} \rightarrow DP$  and  $D^*P$ , while the experimental data are not precise enough to constrain those parameters. The full one- and two-dimensional probability distributions obtained from the fits are summarized in appendix A. In the fit results of  $\bar{B} \rightarrow DP$  and  $D^*P$ , it

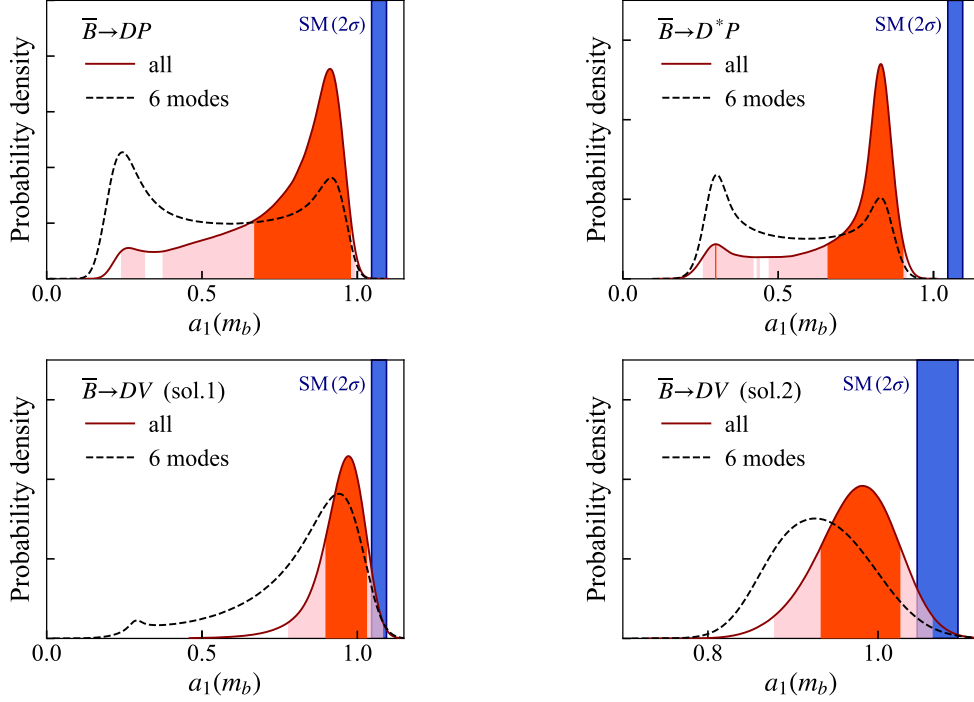


**Figure 5.** Probability distributions of  $a_1(m_b)$ . The darker (lighter) regions correspond to the 68% (95%) probability. The blue vertical band represents the QCDF prediction of  $a_1(m_b)$  at the  $2\sigma$  level.

is observed that there are significant tensions between the theoretical predictions and the experimental data even with including the possible quasi-elastic rescattering effects.

The marginalized one-dimensional probability distributions of  $a_1(m_b)$  in the fits (i) and (ii) are presented in figure 5. Here the result for the solution 2 of  $\bar{B} \rightarrow DV$  is also presented. In each plot the black dotted line shows the result for the fit (i). The distributions for  $\bar{B} \rightarrow DP$  and  $D^*P$  have also a peak in the low  $a_1(m_b)$  region, where  $|a_2^{\text{eff}}|$  is larger than  $a_1(m_b)$  as shown in figure 4. The probability in the low  $a_1(m_b)$  region is suppressed in the fit (ii) as presented by the red-colored distribution. It is found that the preferred regions of  $a_1(m_b)$  differs from the QCDF prediction by more than  $2\sigma$  in  $\bar{B} \rightarrow DP$  and  $D^*P$ , and  $1\sigma$  in  $\bar{B} \rightarrow DV$ .

The NP interpretations of the deviation in  $a_1(m_b)$  are scrutinized in refs. [5, 7, 9, 66]. The NP contributions of  $\mathcal{O}(10\%)$  to the Wilson coefficients  $C_1$  and  $C_2$  have not been excluded by the current measurements of other observables [67–69]. Numerically, the NP contribution to  $a_1(m_b)$  is given in terms of the coefficients at the NP scale, which is taken to be 1 TeV as a reference [9]:

$$a_1^{\text{NP}}(m_b) = -0.19 C_1^{\text{NP}}(1 \text{ TeV}) + 1.07 C_2^{\text{NP}}(1 \text{ TeV}), \quad (3.9)$$

where the renormalization-group evolution is calculated in the leading-logarithmic approximation. In order to achieve  $a_1^{\text{NP}}(m_b) \sim -0.1$ , it is estimated that  $C_2^{\text{NP}}(1 \text{ TeV}) \sim -0.1$  is necessary, which is about 10% of the SM value. Since the SM contribution to  $C_2$  is

generated through a tree-level  $W$ -boson exchange, the requested NP particles must have strong couplings to the light quarks. Such scenarios confront with constraints from LHC, meson mixings and/or  $K$  and also other  $B$  decays [9, 68], and thus, it is challenging in general to construct a viable NP scenario.

## 4 Summary

Recent developments in the study of the  $\overline{B}_{(s)} \rightarrow D_{(s)}$  transition form factors have shed light on the discrepancies between the theoretical predictions and the experimental data for the color-allowed tree decays  $B(\overline{B}^0 \rightarrow D^{(*)+}K^-)$  and  $B(\overline{B}_s^0 \rightarrow D_s^{(*)+}\pi^-)$ . The theoretical predictions for these branching ratios are universally larger than the measured values. On the other hand, it has been known that the decays with the color-suppressed tree amplitude have smaller branching ratios in the factorization approaches than the experimental data. This motivated us to revisit the final-state rescattering effects in the  $\overline{B} \rightarrow DP$ ,  $\overline{B} \rightarrow D^*P$  and  $\overline{B} \rightarrow DV$  channels.

We have examined whether the discrepancies can be explained by the quasi-elastic rescattering contributions based on the  $SU(3)$  and  $U(3)$  flavor symmetries. From the analysis of the color-allowed modes  $\overline{B}^0 \rightarrow D^{(*)+}K^-$  and  $\overline{B}_s^0 \rightarrow D_s^{(*)+}\pi^-$  and the color-suppressed modes  $\overline{B}^0 \rightarrow D^{(*)0}\overline{K}^0$  and  $\overline{B}_s^0 \rightarrow D^{(*)0}\overline{K}^0$ , we have concluded that the rescattering effects cannot account for the discrepancies. Hence there should exist additional contributions such as inelastic rescattering contributions beyond the quasi-elastic picture, large power corrections in the QCDF approach and/or NP contributions to the short-distance Wilson coefficients. We have studied the latter two possibilities by taking the coefficient  $a_1(m_b)$  as a fit parameter. The preferred range of  $a_1(m_b)$  has been determined from the fits to all the available data for  $\overline{B}_{(s)} \rightarrow D_{(s)}^{(*)}M$ , where the fits have been performed separately for  $\overline{B} \rightarrow DP$ ,  $\overline{B} \rightarrow D^*P$  and  $\overline{B} \rightarrow DV$ . The results point to a downward shift of  $\mathcal{O}(10\%)$  in  $a_1(m_b)$  compared to the QCDF prediction. Remarkably, all the fits are consistent with each other.

As argued in detail in ref. [5], it is hard to resolve the discrepancies by (unknown) higher-order or higher-power corrections to the decay amplitudes in the QCDF approach. Effects of the inelastic rescattering might be significant, though their discussion is beyond the scope of this paper. On the other hand, it is also challenging to construct viable NP models that realizes the NP contribution of  $\mathcal{O}(10\%)$ . Therefore, further theoretical and experimental studies are needed to clarify this issue.

## Acknowledgements

We are grateful to Marzia Bordone, Nico Gubernari, Martin Jung and Danny van Dyk for helpful information on their calculation of the  $\overline{B}_{(s)} \rightarrow D_{(s)}$  form factors. We also thank Teppei Kitahara for fruitful discussion. This work is supported in part by the Japan Society for the Promotion of Science under the Grant-in-Aid for Scientific Research on Innovative Areas (No. 21H00086 [ME]), the Grant-in-Aid for Scientific Research B (No. 21H01086 [ME]), the Grant-in-Aid for Early-Career Scientists (No. 16K17681 [ME]),

Research Fellowships for Young Scientists (No. 19J10980 [SI]), Core-to-Core Program (No. JPJSCCA20200002 [SI]), the World Premier International Research Center Initiative [SI], and the Grant-in-Aid for Scientific Research C (No. 17K05429 [SM]). SI would like to thank the warm hospitality at the KEK theory center, where he stayed during the initial stage of this project.

## A Fit results

In this appendix we present some details of the fit results in section 3.3.

Figures 6, 7, 8, and 9 show the one-dimensional and two-dimensional probability distributions of the parameters in the fit (ii), which uses all the available experimental data for  $\bar{B} \rightarrow DP$ ,  $\bar{B} \rightarrow D^*P$ ,  $\bar{B} \rightarrow DV$  with the solution 1 in eq. (2.20), and  $\bar{B} \rightarrow DV$  with the solution 2 in eq. (2.21), respectively. In each plot the darker (lighter) regions correspond to the smallest region of the 68% (95%) probability. There is only a single rescattering parameter  $\delta'$  or  $\sigma$  in the fits to the  $\bar{B} \rightarrow DV$  data, because the  $U(3)$  flavor symmetry is adopted instead of  $SU(3)$ . The results for  $\bar{B} \rightarrow DP$  and  $\bar{B} \rightarrow D^*P$  have a long tail in the one-dimensional distributions of  $a_1(m_b)$ , which corresponds to a large value of  $a_2^{\text{eff}}$ .

In addition, the one-dimensional distributions of  $|E/T_{\text{SM}}|$  are shown in figure 10, where  $T_{\text{SM}}$  is the SM value of the color-allowed tree amplitude for  $\bar{B}^0 \rightarrow D^+K^-$ ,  $\bar{B}^0 \rightarrow D^{*+}K^-$  or  $\bar{B}^0 \rightarrow D^+K^{*-}$ . Here the results in the fits with (without) the rescattering are presented as the distributions in yellow (blue). It is noted that the exchange amplitude  $E$  is power-suppressed compared to the color-allowed tree amplitude [2]. The ranges of  $|E/T_{\text{SM}}|$  in the fits without the rescattering are consistent with the naive power-counting expectation, while a mildly larger value of  $|E/T_{\text{SM}}|$  is allowed in the fits with the rescattering.

Further experimental information on the  $\bar{B}_s$  decays with the  $b \rightarrow c\bar{u}s$  transition listed in tables 1, 2 and 3 is helpful to obtain stronger constraints on the fit parameters, though it would be challenging to measure those decays at the LHCb experiment in most cases. Theoretical studies of the color-suppressed-tree and the exchange amplitudes would also be helpful to set stronger constraints.

## References

- [1] J.D. Bjorken, *Topics in B Physics*, *Nucl. Phys. B Proc. Suppl.* **11** (1989) 325.
- [2] M. Beneke, G. Buchalla, M. Neubert and C.T. Sachrajda, *QCD factorization for exclusive, nonleptonic B meson decays: General arguments and the case of heavy light final states*, *Nucl. Phys. B* **591** (2000) 313 [[hep-ph/0006124](#)].
- [3] C.W. Bauer, D. Pirjol and I.W. Stewart, *A Proof of factorization for  $B \rightarrow D\pi$* , *Phys. Rev. Lett.* **87** (2001) 201806 [[hep-ph/0107002](#)].
- [4] T. Huber, S. Kränkl and X.-Q. Li, *Two-body non-leptonic heavy-to-heavy decays at NNLO in QCD factorization*, *JHEP* **09** (2016) 112 [[1606.02888](#)].
- [5] M. Bordone, N. Gubernari, T. Huber, M. Jung and D. van Dyk, *A puzzle in  $\bar{B}_{(s)}^0 \rightarrow D_{(s)}^+ \{\pi^-, K^-\}$  decays and extraction of the  $f_s/f_d$  fragmentation fraction*, *Eur. Phys. J. C* **80** (2020) 951 [[2007.10338](#)].

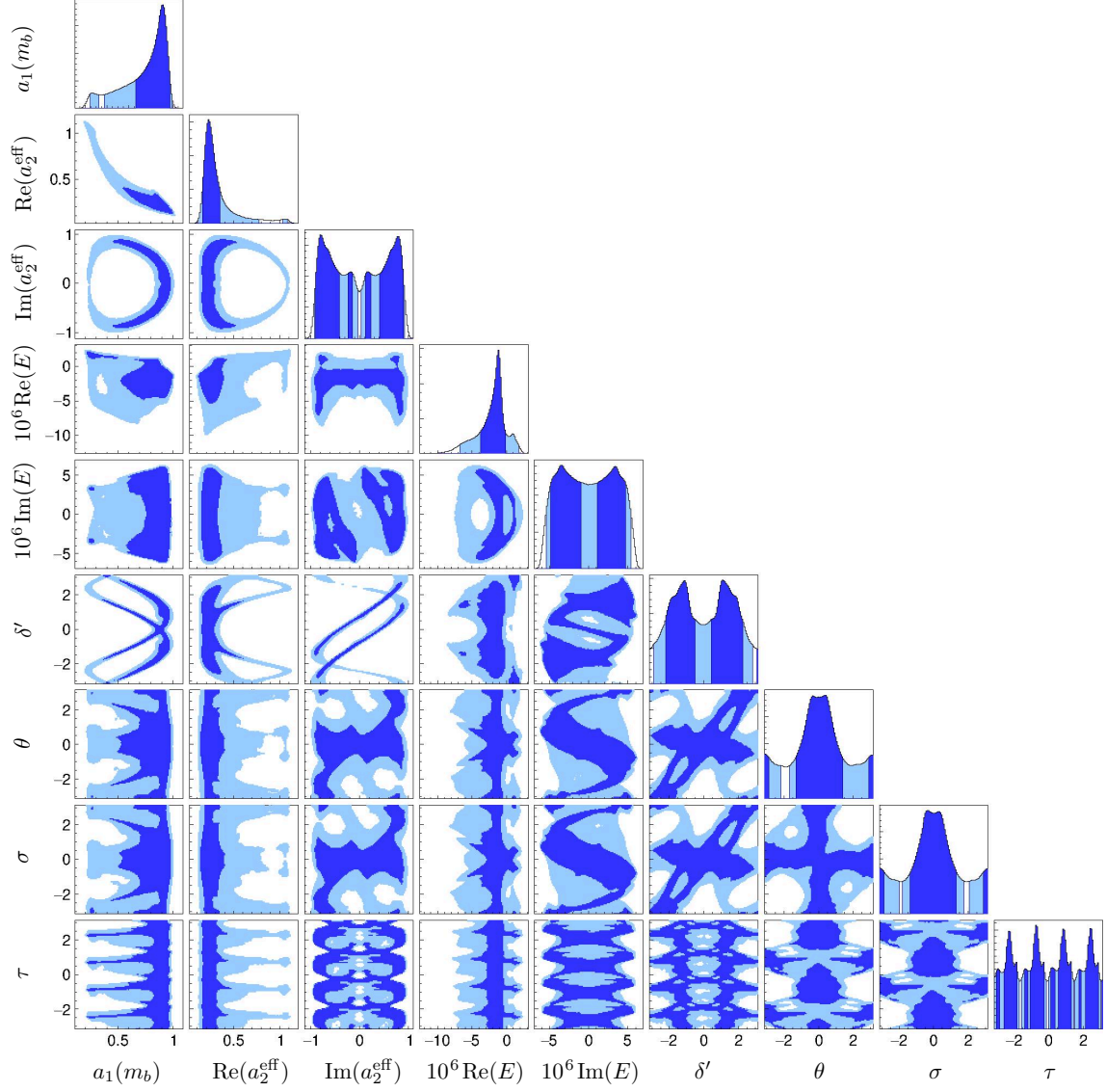


**Figure 6.** Probability distributions of the parameters in  $\bar{B} \rightarrow DP$ . The darker (lighter) regions correspond to the 68% (95%) probability.

- [6] M. Bordone, N. Gubernari, D. van Dyk and M. Jung, *Heavy-Quark expansion for  $\bar{B}_s \rightarrow D_s^{(*)}$  form factors and unitarity bounds beyond the  $SU(3)_F$  limit*, *Eur. Phys. J. C* **80** (2020) 347 [[1912.09335](#)].
- [7] F.-M. Cai, W.-J. Deng, X.-Q. Li and Y.-D. Yang, *Probing new physics in class-I B-meson decays into heavy-light final states*, [2103.04138](#).
- [8] R. Fleischer and E. Malami, *Using  $B_s^0 \rightarrow D_s^\mp K^\pm$  Decays as a Portal to New Physics*, [2109.04950](#).
- [9] S. Iguro and T. Kitahara, *Implications for new physics from a novel puzzle in  $\bar{B}_{(s)}^0 \rightarrow D_{(s)}^{(*)+} \{\pi^-, K^-\}$  decays*, *Phys. Rev. D* **102** (2020) 071701 [[2008.01086](#)].
- [10] H.-Y. Cheng, *Implications of recent  $\bar{B}^0 \rightarrow D^{(*)0} X^0$  measurements*, *Phys. Rev. D* **65** (2002)

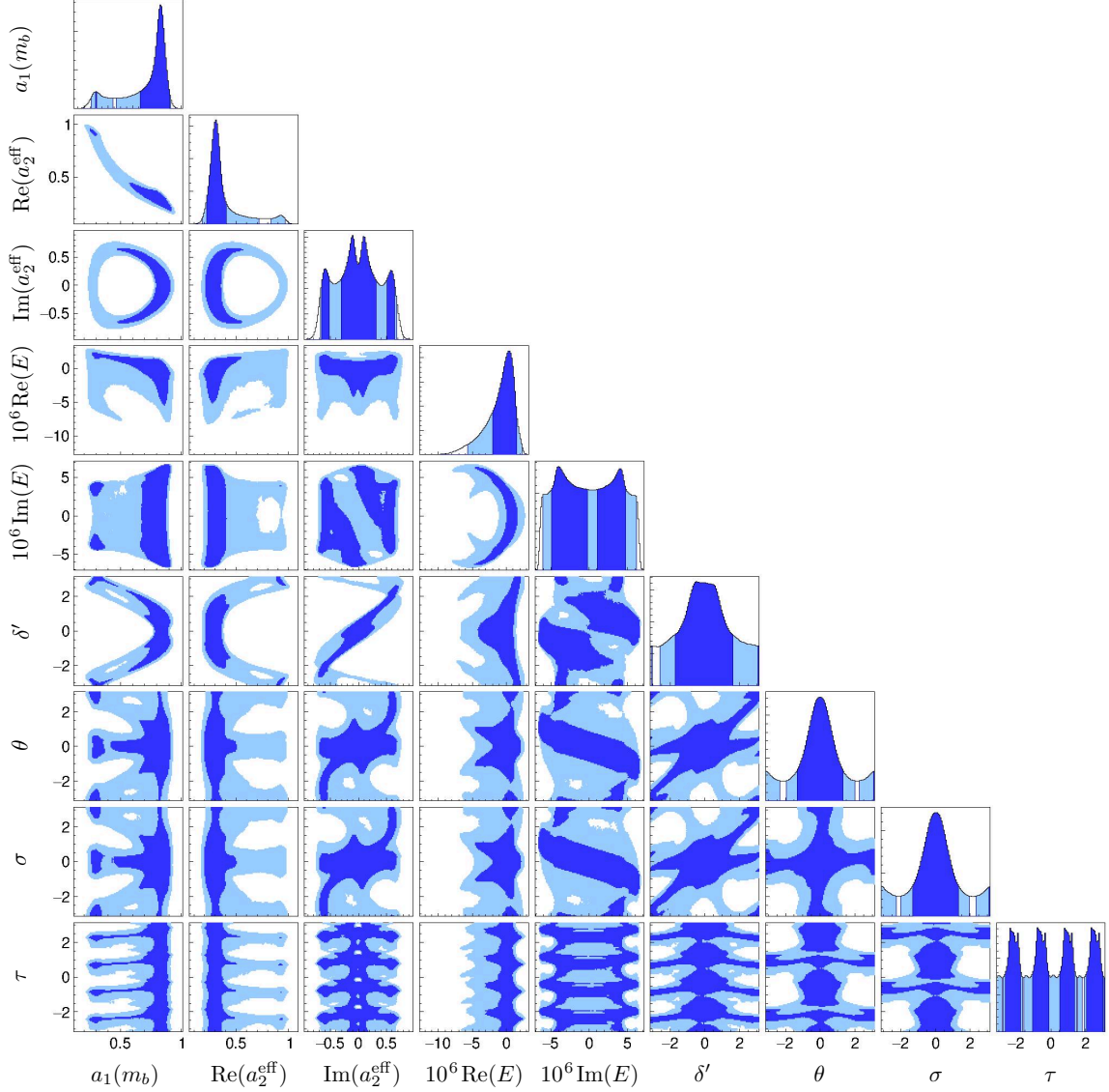


**Figure 7.** Same as figure 6, but for  $\bar{B} \rightarrow D^* P$ .

094012 [[hep-ph/0108096](#)].

- [11] M. Neubert and A.A. Petrov, *Comments on color suppressed hadronic B decays*, *Phys. Lett. B* **519** (2001) 50 [[hep-ph/0108103](#)].
- [12] Z.-z. Xing, *Determining the factorization parameter and strong phase differences in  $B \rightarrow D^{(*)}\pi$  decays*, *HEPNP* **26** (2002) 100 [[hep-ph/0107257](#)].
- [13] Z.-z. Xing, *Final state rescattering and  $SU(3)$  symmetry breaking in  $B \rightarrow DK$  and  $B \rightarrow DK^*$  decays*, *Eur. Phys. J. C* **28** (2003) 63 [[hep-ph/0301024](#)].
- [14] C.-W. Chiang and J.L. Rosner, *Final state phases in  $B \rightarrow D\pi$ ,  $D^*\pi$ , and  $D\rho$  decays*, *Phys. Rev. D* **67** (2003) 074013 [[hep-ph/0212274](#)].
- [15] C.S. Kim, S. Oh and C. Yu, *Strong phase shifts and color-suppressed tree amplitudes in  $B \rightarrow DK^{(*)}$  and  $B \rightarrow D\pi$ ,  $D\rho$  decays*, *Phys. Lett. B* **621** (2005) 259 [[hep-ph/0412418](#)].



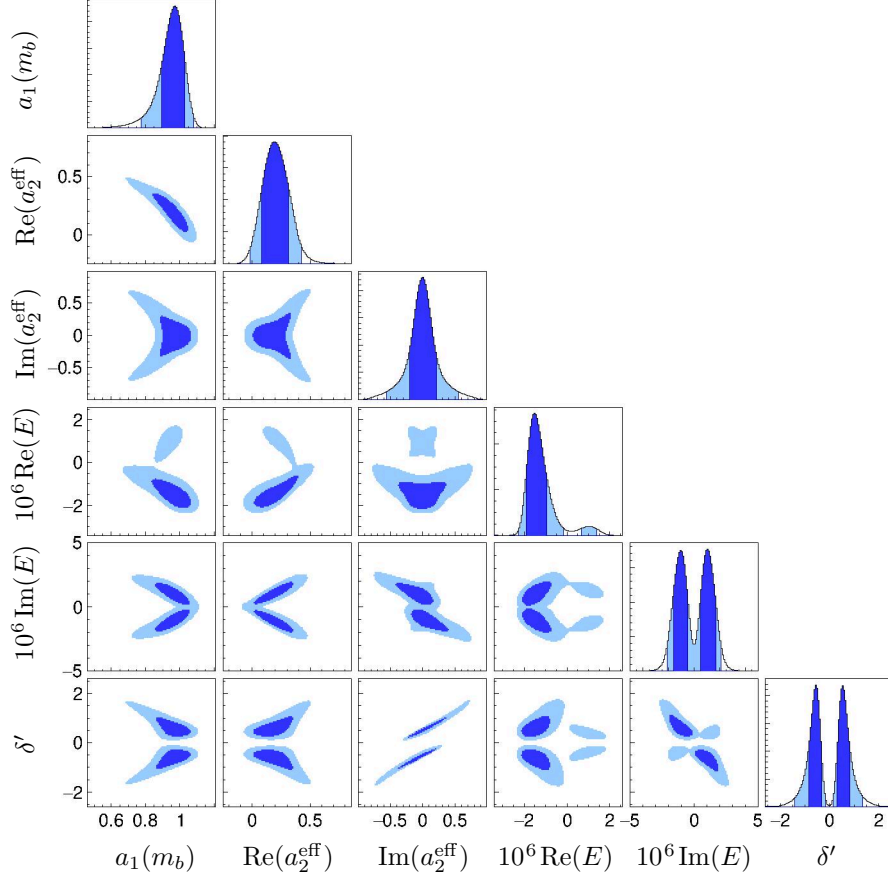


**Figure 8.** Same as figure 6, but for  $\bar{B} \rightarrow DV$  with the solution 1 in eq. (2.20).

- [16] C.-W. Chiang and E. Senaha, *Update analysis of two-body charmed B meson decays*, *Phys. Rev. D* **75** (2007) 074021 [[hep-ph/0702007](#)].
- [17] Y.-Y. Keum, T. Kurimoto, H.N. Li, C.-D. Lu and A.I. Sanda, *Nonfactorizable contributions to  $B \rightarrow D^{(*)}M$  decays*, *Phys. Rev. D* **69** (2004) 094018 [[hep-ph/0305335](#)].
- [18] R.-H. Li, C.-D. Lu and H. Zou, *The  $B(B_s) \rightarrow D_s P, D_s V, D_s^* P$  and  $D_s^* V$  decays in the perturbative QCD approach*, *Phys. Rev. D* **78** (2008) 014018 [[0803.1073](#)].
- [19] B.Y. Blok and M.A. Shifman, *Weak Nonleptonic Decays of Charmed Mesons: Theory Versus Experiment*, *Sov. J. Nucl. Phys.* **45** (1987) 522.
- [20] S. Mantry, D. Pirjol and I.W. Stewart, *Strong phases and factorization for color suppressed decays*, *Phys. Rev. D* **68** (2003) 114009 [[hep-ph/0306254](#)].
- [21] A.E. Blechman, S. Mantry and I.W. Stewart, *Heavy quark symmetry in isosinglet nonleptonic B-decays*, *Phys. Lett. B* **608** (2005) 77 [[hep-ph/0410312](#)].
- [22] I.E. Halperin, *Soft gluon suppression of  $1/N_c$  contributions in color suppressed heavy meson decays*, *Phys. Lett. B* **349** (1995) 548 [[hep-ph/9411422](#)].
- [23] J.-Y. Cui and Z.-H. Li, *Soft nonfactorizable contribution to  $\bar{B}^0 \rightarrow D^0 \pi^0$* , *Eur. Phys. J. C* **38** (2004) 187 [[hep-ph/0410029](#)].

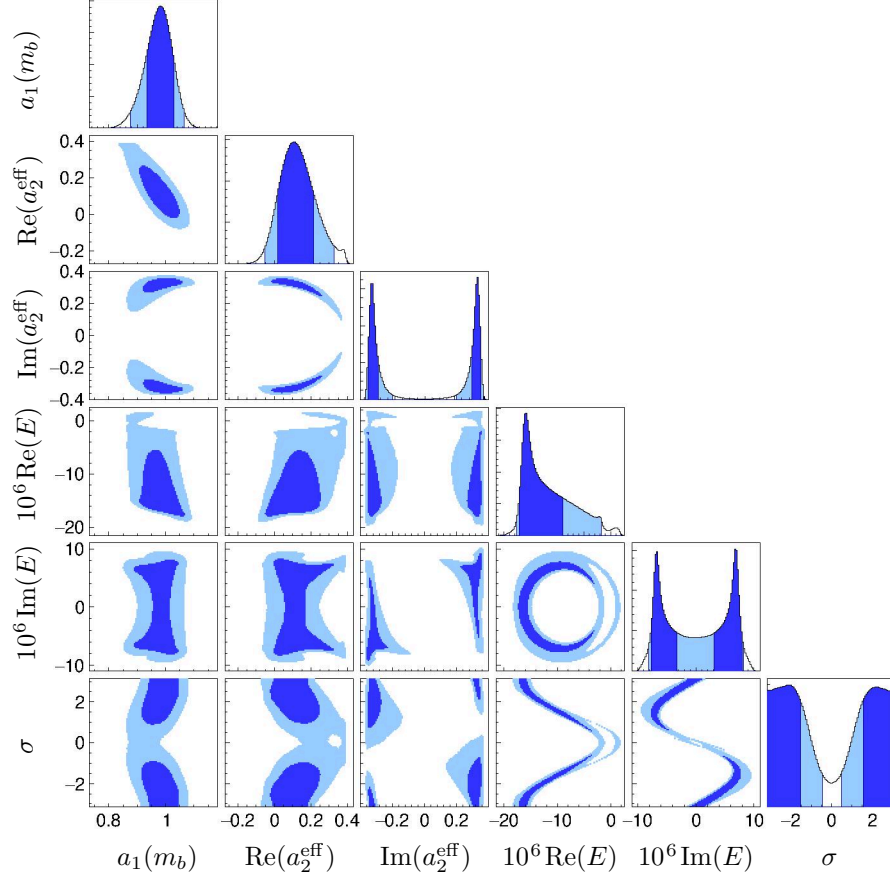


**Figure 9.** Same as figure 6, but for  $\bar{B} \rightarrow DV$  with the solution 2 in eq. (2.21).

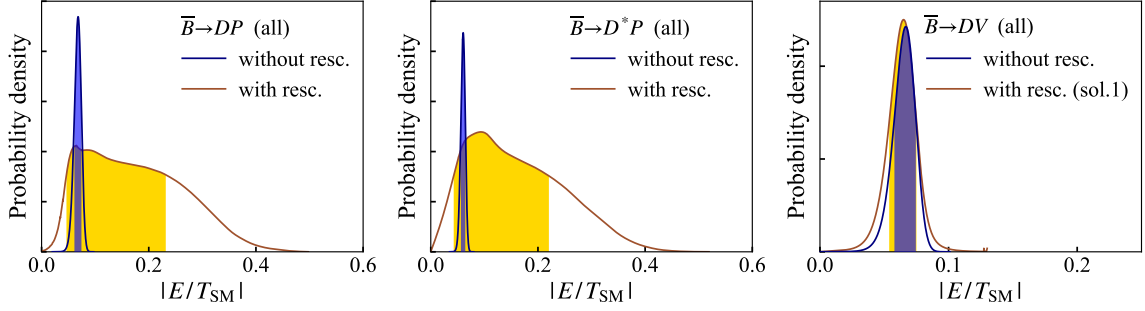


**Figure 10.** Probability distributions of  $|E/T_{\text{SM}}|$ . The colored regions correspond to 68% probability.

- [24] J.F. Donoghue, E. Golowich, A.A. Petrov and J.M. Soares, *Systematics of soft final state interactions in B decay*, *Phys. Rev. Lett.* **77** (1996) 2178 [[hep-ph/9604283](#)].
- [25] B. Blok and I.E. Halperin, *Regge asymptotics and color suppressed heavy meson decays*, *Phys. Lett. B* **385** (1996) 324 [[hep-ph/9605441](#)].
- [26] M. Suzuki and L. Wolfenstein, *Final state interaction phase in B decays*, *Phys. Rev. D* **60** (1999) 074019 [[hep-ph/9903477](#)].



- [27] C.-K. Chua, W.-S. Hou and K.-C. Yang, *Final state rescattering and color suppressed  $\overline{B}^0 \rightarrow D^{(*)0} h^0$  decays*, *Phys. Rev. D* **65** (2002) 096007 [[hep-ph/0112148](#)].
- [28] Fayyazuddin, *Final state interactions and  $\Delta S = -1$ ,  $\Delta C = \pm 1$   $B$  decays*, *JHEP* **09** (2002) 055 [[hep-ph/0206164](#)].
- [29] L. Wolfenstein, *Strong phases in the decays  $B \rightarrow D\pi$* , *Phys. Rev. D* **69** (2004) 016006 [[hep-ph/0309166](#)].
- [30] G. Calderon, J.M. Gerard, J. Pestieau and J. Weyers, *Relating final state interactions in  $B \rightarrow D\pi$  and  $B \rightarrow DK$* , *Phys. Lett. B* **588** (2004) 81 [[hep-ph/0311163](#)].
- [31] Fayyazuddin, *Final state phases in  $B \rightarrow D\pi$ ,  $\overline{D}\pi$  decays and CP asymmetry*, *Phys. Rev. D* **70** (2004) 114018 [[hep-ph/0402189](#)].
- [32] L. Wolfenstein, *Regge amplitudes and final state phases in the decays  $B \rightarrow D\pi$* , [[hep-ph/0407344](#)].
- [33] H.-Y. Cheng, C.-K. Chua and A. Soni, *Final state interactions in hadronic  $B$  decays*, *Phys. Rev. D* **71** (2005) 014030 [[hep-ph/0409317](#)].
- [34] C.-K. Chua and W.-S. Hou, *Implications of  $\overline{B} \rightarrow D^0 h^0$  decays on  $\overline{B} \rightarrow D\overline{K}$ ,  $\overline{D}\overline{K}$  decays*, *Phys. Rev. D* **72** (2005) 036002 [[hep-ph/0504084](#)].
- [35] C.-K. Chua and W.-S. Hou, *Rescattering effects in  $\overline{B}_{u,d,s} \rightarrow DP$ ,  $\overline{D}P$  decays*, *Phys. Rev. D* **77** (2008) 116001 [[0712.1882](#)].
- [36] M. Suzuki, *Inelastic final-state interaction*, *Phys. Rev. D* **77** (2008) 054021 [[0710.5534](#)].
- [37] S. Iguro and R. Watanabe, *Bayesian fit analysis to full distribution data of  $\overline{B} \rightarrow D^{(*)} \ell \overline{\nu} : |V_{cb}|$  determination and new physics constraints*, *JHEP* **08** (2020) 006 [[2004.10208](#)].
- [38] A. Kobach, *Continuity and semileptonic  $B_{(s)} \rightarrow D_{(s)}$  form factors*, *Phys. Lett. B* **809** (2020) 135708 [[1910.13024](#)].
- [39] PARTICLE DATA GROUP collaboration, *Review of Particle Physics*, *PTEP* **2020** (2020) 083C01.
- [40] N. Cabibbo, *Unitary Symmetry and Leptonic Decays*, *Phys. Rev. Lett.* **10** (1963) 531.
- [41] M. Kobayashi and T. Maskawa, *CP Violation in the Renormalizable Theory of Weak Interaction*, *Prog. Theor. Phys.* **49** (1973) 652.
- [42] K.G. Chetyrkin, M. Misiak and M. Munz, *Weak radiative  $B$  meson decay beyond leading logarithms*, *Phys. Lett. B* **400** (1997) 206 [[hep-ph/9612313](#)].
- [43] K.G. Chetyrkin, M. Misiak and M. Munz,  *$|\Delta F| = 1$  nonleptonic effective Hamiltonian in a simpler scheme*, *Nucl. Phys. B* **520** (1998) 279 [[hep-ph/9711280](#)].
- [44] C.-K. Chua, *Revisiting final state interaction in charmless  $B_q \rightarrow PP$  decays*, *Phys. Rev. D* **97** (2018) 093004 [[1802.00155](#)].
- [45] D. Zeppenfeld,  *$SU(3)$  Relations for  $B$  Meson Decays*, *Z. Phys. C* **8** (1981) 77.
- [46] M.J. Savage and M.B. Wise,  *$SU(3)$  Predictions for Nonleptonic  $B$  Meson Decays*, *Phys. Rev. D* **39** (1989) 3346.
- [47] M. Gronau, O.F. Hernandez, D. London and J.L. Rosner, *Broken  $SU(3)$  symmetry in two-body  $B$  decays*, *Phys. Rev. D* **52** (1995) 6356 [[hep-ph/9504326](#)].

- [48] P. Colangelo and R. Ferrandes, *Model independent analysis of a class of  $\overline{B}_s^0$  decay modes*, *Phys. Lett. B* **627** (2005) 77 [[hep-ph/0508033](#)].
- [49] R. Fleischer, N. Serra and N. Tuning, *Tests of Factorization and  $SU(3)$  Relations in  $B$  Decays into Heavy-Light Final States*, *Phys. Rev. D* **83** (2011) 014017 [[1012.2784](#)].
- [50] R. Escribano, S. González-Solís, P. Masjuan and P. Sanchez-Puertas,  *$\eta'$  transition form factor from space- and timelike experimental data*, *Phys. Rev. D* **94** (2016) 054033 [[1512.07520](#)].
- [51] HFLAV collaboration, *Averages of  $b$ -hadron,  $c$ -hadron, and  $\tau$ -lepton properties as of 2018*, *Eur. Phys. J. C* **81** (2021) 226 [[1909.12524](#)].
- [52] N. Gubernari, A. Kokulu and D. van Dyk,  *$B \rightarrow P$  and  $B \rightarrow V$  Form Factors from  $B$ -Meson Light-Cone Sum Rules beyond Leading Twist*, *JHEP* **01** (2019) 150 [[1811.00983](#)].
- [53] A. Bazavov et al.,  *$B$ - and  $D$ -meson leptonic decay constants from four-flavor lattice QCD*, *Phys. Rev. D* **98** (2018) 074512 [[1712.09262](#)].
- [54] FLAVOUR LATTICE AVERAGING GROUP collaboration, *FLAG Review 2019: Flavour Lattice Averaging Group (FLAG)*, *Eur. Phys. J. C* **80** (2020) 113 [[1902.08191](#)].
- [55] A. Bharucha, D.M. Straub and R. Zwicky,  *$B \rightarrow V\ell^+\ell^-$  in the Standard Model from light-cone sum rules*, *JHEP* **08** (2016) 098 [[1503.05534](#)].
- [56] P. Gelhausen, A. Khodjamirian, A.A. Pivovarov and D. Rosenthal, *Decay constants of heavy-light vector mesons from QCD sum rules*, *Phys. Rev. D* **88** (2013) 014015 [[1305.5432](#)].
- [57] P. Ball and R. Zwicky, *New results on  $B \rightarrow \pi, K, \eta$  decay formfactors from light-cone sum rules*, *Phys. Rev. D* **71** (2005) 014015 [[hep-ph/0406232](#)].
- [58] G. Duplancic and B. Melic, *Form factors of  $B, B_s \rightarrow \eta^{(\prime)}$  and  $D, D_s \rightarrow \eta^{(\prime)}$  transitions from QCD light-cone sum rules*, *JHEP* **11** (2015) 138 [[1508.05287](#)].
- [59] A. Khodjamirian and A.V. Rusov,  *$B_s \rightarrow K\ell\nu_\ell$  and  $B_{(s)} \rightarrow \pi(K)\ell^+\ell^-$  decays at large recoil and CKM matrix elements*, *JHEP* **08** (2017) 112 [[1703.04765](#)].
- [60] BELLE collaboration, *Precise determination of the CKM matrix element  $|V_{cb}|$  with  $\overline{B}^0 \rightarrow D^{*+}\ell^-\bar{\nu}_\ell$  decays with hadronic tagging at Belle*, [1702.01521](#).
- [61] BELLE collaboration, *Measurement of the CKM matrix element  $|V_{cb}|$  from  $B^0 \rightarrow D^{*-}\ell^+\nu_\ell$  at Belle*, *Phys. Rev. D* **100** (2019) 052007 [[1809.03290](#)].
- [62] M. Beneke, P. Böer, G. Finauri and K.K. Vos, *QED factorization of two-body non-leptonic and semi-leptonic  $B$  to charm decays*, [2107.03819](#).
- [63] J. De Blas et al., *HEPfit: a code for the combination of indirect and direct constraints on high energy physics models*, *Eur. Phys. J. C* **80** (2020) 456 [[1910.14012](#)].
- [64] A. Caldwell, D. Kollar and K. Kroninger, *BAT: The Bayesian Analysis Toolkit*, *Comput. Phys. Commun.* **180** (2009) 2197 [[0808.2552](#)].
- [65] LHCb collaboration, *Measurement of CP observables in  $B^\pm \rightarrow D^{(*)}K^\pm$  and  $B^\pm \rightarrow D^{(*)}\pi^\pm$  decays using two-body  $D$  final states*, *JHEP* **04** (2021) 081 [[2012.09903](#)].
- [66] M. Bordone, A. Greljo and D. Marzocca, *Exploiting dijet resonance searches for flavor physics*, [2103.10332](#).
- [67] C. Bobeth, U. Haisch, A. Lenz, B. Pecjak and G. Tetlalmatzi-Xolocotzi, *On new physics in  $\Delta\Gamma_d$* , *JHEP* **06** (2014) 040 [[1404.2531](#)].

- [68] J. Brod, A. Lenz, G. Tetlalmatzi-Xolocotzi and M. Wiebusch, *New physics effects in tree-level decays and the precision in the determination of the quark mixing angle  $\gamma$* , *Phys. Rev. D* **92** (2015) 033002 [[1412.1446](#)].
- [69] A. Lenz and G. Tetlalmatzi-Xolocotzi, *Model-independent bounds on new physics effects in non-leptonic tree-level decays of B-mesons*, *JHEP* **07** (2020) 177 [[1912.07621](#)].